Fisheries Research 279 (2024) 107125

Contents lists available at ScienceDirect

Fisheries Research

journal homepage: www.elsevier.com/locate/fishres

Review

Fisheries at Lagrangian fronts

S.V. Prants [1]

V.I. Il'ichev Pacific Oceanological Institute of the Russian Academy of Sciences, 43 Baltiyskaya St, Vladivostok 690041, Russia

ARTICLE INFO

Keywords:
Overview
Lagrangian and ocean fronts
Fisheries
Indicators of water motion

ABSTRACT

This paper reviews the recent progress in the application of Lagrangian methods for detecting potential feeding and fishing grounds and the relationship between the dynamic features with strong gradients of the relevant indicators of water motion, Lagrangian fronts (LFs), and catches of different species of pelagic fish and squid. The locations of the LFs, approximating locations of the ocean features with increased values of the gradients of hydrological parameters, can be calculated by solving advection equations for a large number of virtual passive particles in the altimetric velocity field or in the velocity fields generated by numerical circulation models or obtained using high-frequency radars. The LFs can be easily identified in the near real time, under any weather conditions and in the areas with small contrasts of sea surface temperature. The proximity of catch sites to location of LFs has been shown with the help of statistical tests in different seas and oceans based on catch reports of fishing vessels. The active and passive physical mechanisms at fronts, that may provide favorable conditions for foraging and feeding, are discussed. The paper emphasizes the importance of fronts in marine ecology and sustainable fisheries.

1. Introduction

One of the reasons for the heterogeneity and patchiness of marine biomass distribution is the dynamic nature of the environment with currents, intrusions, upwelling zones and eddies, which transport and redistribute water masses and affect their properties over a large range of spatial and temporal scales (e.g., Bertrand, et al., 2014). Identifying the factors, that underlie that patchiness, is fundamental to understanding how they affect marine ecosystem stability. Human activity impacts strongly on this stability and sustainability of marine resources. As to fishery, the spatial distribution of fishing efforts is important to the organization of marine food webs (e.g., Essington et al., 2006) and to sustainability of fisheries (e.g., Basson, 1999; Murawski et al., 2005, Fulton et al., 2011). Almost all fishery management actions are designed to influence the spatial and temporal behavior of fishermen (e.g., Branch et al., 2006; Hilborn, 2007). On the one hand, their behavior is motivated by a desire to maximize profit, but on the other hand, there is a risk of overfishing. The issue of where and when fishermen decide to fish remains an important factor to achieving sustainable fisheries (e.g., Fulton et al., 2011; Hobday et al., 2011; Hobday and Hartog. 2014).

Captains of fishing vessels often use satellite-derived maps of sea surface temperature (SST) to identify the ocean (hydrological) fronts with sharp thermal gradients and to decide where to fish based on the location of the frontal features. The strong fronts are characterized by a confluence of waters with different properties (Reid et al., 1978; Le Févre, 1987; Owen, 1981; Olson and Backus, 1985; Franks, 1992a and 1992b; Sournia, 1994; Olson et al., 1994; Polovina et al., 2001; Palacios et al., 2006; Bakun, 2006; Lehahn et al., 2007; Ainley et al., 2009; Belkin and O'Reilly, 2009; Lévy et al., 2012, 2018; Kahru et al., 2012; Godø et al., 2012; Prants et al., 2012, 2014, 2021; Hobday and Hartog, 2014; Kida et al., 2015; Scales et al., 2018; Lehahn et al., 2018; Watson et al., 2018; De Verneil et al., 2019). These transient ocean features promote aggregation of nutrients, phytoplankton and zooplankton growth in oligotrophic waters contributing to creation of oases of marine life in the oceanic desert for marine habitants, from small pelagic fish to seabirds and top predators (Olson et al., 1994; Weimerskirch et al., 2004; Bakun, 2006; Bost et al., 2009; Tew Kai et al., 2009; Ainley et al., 2009; Dunn et al., 2011; Prants et al., 2012, 2014, 2021; Godø et al., 2012; De Monte et al., 2012; Scales et al., 2014; Chen et al., 2014; Woodson and Litvin, 2015; Snyder et al., 2017; Hernández-Carrasco et al., 2020; Kulik et al., 2022; Mangolte et al., 2023; Ito et al., 2023).

The fronts and frontal eddies play an important role in the development of potential fish habitats by creating hydrodynamic 'traps' of prey and good feeding opportunities through local enhancement of zooplankton abundance and aggregation of prey organisms (Olson and Backus, 1985; Myers and Drinkwater, 1989; Sugimoto and Tameishi,

E-mail address: prants@poi.dvo.ru.
[1] URL: http: // dynalab. poi. dvo. ru,

https://doi.org/10.1016/j.fishres.2024.107125
Received 1 April 2024; Received in revised form 26 June 2024; Accepted 26 July 2024
Available online 30 July 2024

1992; Yasuda and Watanabe, 1994; Logerwell and Smith, 2001; Kasai et al., 2002; Okazaki et al., 2002; Bakun, 2006; Prants et al., 2012, 2014, Prants, 2013; Belkin et al., 2014; Chen et al., 2014; Tseng et al., 2014; Budyansky et al., 2017; 2022; Scales et al., 2018; Watson et al., 2018; Baudena et al., 2021; Kulik et al., 2022, Mangolte et al., 2023; Suthers et al., 2023).

Accurate detection of oceanic fronts requires *in situ* measurements at a dense grid of stations that is very expensive and practically impossible on a global scale. SST and SSH satellite imagery is commonly used to map ocean fronts globally (e.g., Legeckis, 1978; Miller, 2009) including automatic front identification algorithms (e.g., Belkin and O'Reilly, 2009; Belkin et al., 2014 and Belkin, 2021; Xing et al., 2023). Fishermen routinely use SST images in detecting fronts. However, cloudiness, low thermal contrasts in warm seasons, flow discontinuities, noise and low spatial resolution of some satellite data present challenges for identifying the location of ocean fronts (Ullman and Cornillon, 2000; Miller, 2009). Detecting fronts in satellite images manually is a tedious and subjective task. The required time period to get a clear view of the ocean may be a few days or more than a month depending on the cloudiness of the region. Conventional compositing methods average all cloud-free values obtained for each location, to produce a coarse distribution of temperature or chl-a. Analyses of mesoscale features, averaging all cloud-free values obtained for each location, are of little value, because any dynamic aspects will be blurred in the time-averaged composite (Miller, 2009).

After 1997, when SeaWiFS ocean color imagery became available (https://oceancolor.gsfc.nasa.gov/SeaWiFS), there appeared the possibility to map ocean fronts monitoring chlorophyll-a (chl-a) concentration from space. However, the same front may appear quite differently in chl-a field and in SST and sea surface height (SSH) images (Miller, 2009; Belkin et al., 2009). The reason is in the inherent complexity of chl-a field evident from ocean color imagery and from *in situ* data. The patterns with chl-a blooms and patchiness is a product of interplay of physical, chemical, and biological processes, and therefore are inherently more complex than the structure of SST and SSH fronts.

To overcome these challenges, the alternative approach has been developed in the recent decades for capturing frontal features based on the extraction of Lagrangian structures in chaotic oceanic flows. In this approach, the relevant indicators of water motion are computed to provide information on the origin, advection history, 'age' and other kinematic properties of water masses (Prants et al., 2011, 2012, 2014; 2015a; Sanial et al., 2014), on the location of barriers to transport (Boffetta et al., 2001), and on the location of Lagrangian coherent structures (LCS, Haller, 2002, 2015).

Being motivated by the idea to find other than SST and chl-a indicators of the presence of ocean fronts that can be easily computed in a given velocity field, the concept of LFs was proposed by Prants et al. (2012), (2014). By definition, LF is a boundary with the strong horizontal gradient of the relevant Lagrangian indicator that is a function of particle trajectories. The studies of connection of LFs with potential fishing grounds have begun in those papers. Moreover, the LFs have been shown to influence movement of southern elephant seals (d'Ovidio et al., 2013; Cotté et al., 2015), penguins (Sanial et al., 2014) and wales (Fahlbusch et al., 2022) optimizing energy efforts in searching for food (Abrahms, 2018).

This review is the first survey of achievements in the Lagrangian diagnostics of open-ocean fronts with the focus on the role of LFs for fisheries. Section 2 introduces some indicators for detecting LFs in oceanic flows. The review of the results on fisheries at the LF boundaries in the northwestern Pacific Ocean, in the Okhotsk Sea, in California Current System, in Mediterranean Sea and larval ecology is contained in Section 3. A comparison of acoustic *in situ* measurements of mesopelagic fish concentration with the satellite derived LFs in the Southern Ocean is presented in Section 4. The significance of active and passive fronts in fisheries is discussed in Section 5, and the conclusions are provided in Sec. 6.

2. 2. Detecting fronts with the help of Lagrangian indicators

2.1. 2.1. Identification of stationary points in oceanic flows

In the Lagrangian approach, the transport processes are tracked by following fluid parcels carrying salt, heat, nutrients, plankton and other particulate matter (see for a review Griffa et al., 2007; Prants et al., 2017; van Sebille et al., 2018). A large number of artificial particles, representing water parcels, are numerically advected in the satellite-derived altimetric velocity field or in the velocity fields of circulation models/reanalyses in order to detect ocean fronts in chaotic oceanic flows. The mesoscale features in the ocean are reliably identified in the altimetric velocity field (one of the AVISO/CMEMS products \url {aviso.altimetry.fr}) with the resolution of 0.25° x 0.25° and daily time step.

The values of velocity vanish at stationary (fixed) points in a flow. By the type of stability, they are divided into two classes: elliptic and hyperbolic points. These points are the main controlling objects of the flow. They are moving objects in unsteady flows. Elliptic (stable) points are usually located within eddies, where rotation prevails over deformation. Hyperbolic (unstable) points are located around the vortex cores, where deformation prevails over rotation. The stationary points are identified daily in the altimetry-based velocity field and more frequently in the velocity fields of numerical circulation models. As to elliptic points approximating the location of eddy centers, the comparison of the altimetry-based simulation results with the location of the eddy centers defined from CTD sections across mesoscale eddies during a few R/V cruises has shown good correspondence with the accuracy of the order of 5–10 km (e.g., Prants et. al, 2016, 2018, 2020). This accuracy is better than the nominal resolution of the altimetry data due to smoothness of the AVISO velocity fields within eddies.

The validation of locations of hyperbolic points is more problematic because there are no evident oceanographic features associated with these points. The hyperbolic points can be strictly defined as the null-dimensional objects where the associated stable and unstable manifolds intersect each other (see the text below). The validation of locations of these points in the altimetric velocity fields can be performed looking at trajectories of drifters accidentally got into the neighborhood of a hyperbolic point (e.g., Buesseler et al., 2012; Prants et al., 2015b and 2016; Nishikawa et al., 2021).

2.2. 2.2. Lagrangian indicators of water motion

A number of Lagrangian indicators of water motion, which are functions of particle trajectories, have been introduced by Prants et al. (2011), (2014), (2017), (2018), Sanial et al. (2014), d'Ovidio et al. (2015), Cotté et al. (2015), Della Penna et al. (2017), Lehahn et al. (2018), Ponomarev et al. (2018), Fifani et al. (2021). Calculating these indicators in a given velocity field and depicting their values on geographic maps of a study area, one gets the Lagrangian maps where the LFs can be identified as lines in 2D flows (or surfaces in 3D flows) with the maximum (local) gradients of the relevant indicators. The commonly used Lagrangian indicator for quantifying chaotic mixing and transport is the finite-time Lyapunov exponent (FTLE) accumulated over a certain period of time $t - t_0$. FTLE may be calculated by different ways, for example, using the finite-time Cauchy–Green deformation tensor (Shadden et al., 2005) or the evolution matrix (Prants et al., 2011):

$$\Lambda(\mathrm{t}, \mathrm{t}_0) = \frac{\ln\sigma(\mathrm{t}, t_0)}{t - t_0}, \#(1)$$

where $\sigma(t,t_0)$ is the maximum singular value of the evolution matrix. The FTLE values measure the maximum separation of close-by particles after a finite advection time. Some authors use the finite-size Lyapunov exponent (FSLE), computed until a certain specified distance between pairs of initially close-by particles is reached (e.g., Boffetta et al., 2001;

d'Ovidio et al., 2004)

$$\Lambda_s = \frac{\ln(\delta_f/\delta_0)}{\tau}.\#(2)$$

The values of Λ_s are calculated by integrating the advection equations until the time moment τ, when two particles, initially separated by a distance δ_0, diverge over a distance δ_f from each other. The FSLE and FTLE diagnostics give similar results in detecting Lagrangian structures. The 'ridges' with maximum (local) FTLE/FSLE values, calculated backward in time, approximate the location of the so-called unstable manifolds, whereas the maximum Lyapunov values, calculated forward in time, approximate the location of the so-called stable manifolds (Pierrehumbert, 1991; Haller, 2002 and 2015). These invariant manifolds play the important role in the organization of chaotic flows forming a kind of a skeleton. The instantaneous position of a moving hyperbolic point is defined by the crossing point of backward- and forward-in-time FTLE/FSLE 'ridges'.

Computing the length of particle trajectories, L, (Mendoza and Mancho, 2010; Ponomarev et al., 2018), it is possible to delineate vortex contours and to document the processes of entrainment and detrainment of water by eddies (Prants et al., 2018). The origin or O-maps (Lipphardt et al., 2006; Prants et al., 2014 and 2018; Rwawi et al., 2024) are used to identify the origin of water masses converging at fronts. The indicator of the residence time of water (Nauman, 2008) is helpful in detecting frontal features in the areas with intrusions of a foreign water into a basin (Budyansky et al., 2022). The Λ, O, L and residence-time maps are parameterized by a starting date and an integration period and provide us with complementary information on the movement of water masses.

2.3. 2.3. Identification of Lagrangian fronts

Ocean front is a relatively narrow zone with enhanced horizontal gradients of temperature, salinity, density and, sometimes, with distinct biological properties on either side of the front (nutrients, concentrations of chl-a and phytoplankton) that are much stronger than the background. Large-scale ocean fronts separate, as a rule, water masses of distinct origin. Any ocean front is an Eulerian feature existing in this place at this time. A Lagrangian front is both an Eulerian feature, since it is a frontal boundary, and a Lagrangian structure, since it is defined by large horizontal gradients of the relevant Lagrangian indicators that can be calculated in a given velocity field.

The fields of Lagrangian indicators contain information not only on 'instantaneous' characteristics of water mass and positions of ocean fronts but also on advection history and origin of water masses converging at fronts (Prants et al., 2014). Even if distinct frontal water masses are almost indistinguishable in SST infrared images (the SST contrast is small), the corresponding LFs can be identified on the maps of the relevant indicators. It is important for fisheries because the potential fishing grounds can be distinguished among a variety of frontal zones present in the study area. Thus, calculation of the LF locations allows us to detect dynamic frontal features and their evolution in any weather, to get information about the history and origin of converging water masses and to estimate oceanographic conditions favorable for feeding of different species of pelagic fish and other sea habitants.

Fig. 1 illustrates schematically by which way fish can aggregate at a LF. As it follows from dynamical system theory, the so-called stable W_s and unstable W_u invariant manifolds are associated with hyperbolic points which are unstable fixed points in a flow (e.g., Ottino, 1989; Wiggins, 1992). W_s and W_u are transport barriers that minimize advection across manifolds and maximize it along them. These structures, hidden in a flow, can be visualized in laboratory experiments with a dye (Ottino, 1989). In the ocean, the unstable manifolds may appear on satellite images of the ocean color where chl-a filaments and swirls indicate their location (e.g., Lehahn et al., 2007; d'Ovidio et al., 2010). The presence of stable and unstable manifolds sometimes is manifested in trajectories of drifting buoys in the ocean (e.g., Buesseler et al., 2012; Prants et al., 2015b and 2016; Nishikawa et al., 2021).

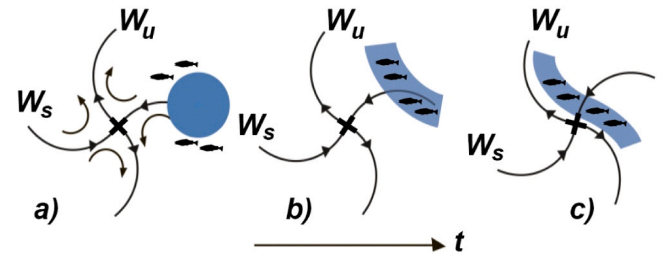

Fig. 1. Illustration of the influence of Lagrangian front on the behavior of fish. The black curves schematically show stable W_s and unstable W_u manifolds of the hyperbolic point (cross). The school of fish follows the patch rich in food (a). After a certain amount of time, the patch will be compressed across the direction of the unstable manifold and enlarged along it due to stirring (b). The fish follow the patch and aggregate along the LF (c). After exhaustion of the food supply, fish disperse again.

A circular tracer patch in the proximity of a distinguished hyperbolic point, identified by the large values of FTLE or FSLE, is typically compressed along its stable manifold and elongated along the unstable one (Fig. 1). Eventually, diffusion acts on the thinning of the tracer by dissipating it and reducing the tracer concentration until it is below the threshold detected by the fish. If we suppose that fish are interested in the area with high values of the tracer (food) concentration, they will swim to follow the contracting patch and aggregate along the corresponding LF.

The terms 'strong/weak LF' and 'permanent/ephemeral LFs are used in order to distinct fronts with large/small values of horizontal gradients of Lagrangian indicators and long/short existence time of fronts, respectively. Moreover, the terms 'active' and 'passive' fronts are used in this paper in order to differ active and passive mechanisms by which the corresponding fronts drive biological processes (Lévy et al., 2018). A frontal feature, for which the gradient in density is large enough to sustain enhanced vertical nutrient fluxes may be considered as an active LF. Passive LF is a frontal feature with large horizontal values of gradients of concentrations of chl-a or phytoplankton or large horizontal values of gradients of specific properties of water like 'age' and/or the residence/retention time. The vertical fluxes are typically small at passive fronts. The tracer patches in the surface mixed layer just stir horizontally by large-scale currents. Some passive LFs can be seen on satellite images of ocean color and SST (see, e.g., Lehahn et al., 2007 and 2018; d'Ovidio et al., 2010 and 2013; Budyansky et al., 2022).

Lagrangian front was defined by Prants et al. (2012) and, (2014) as a line or surface with the large gradient values of a relevant Lagrangian indicator. This definition contains also the method for calculating locations of LFs. Lagrangian coherent structures (LCSs) are exceptional material surfaces that exert a major influence on nearby trajectories over a time interval of interest (Haller, 2002 and 2015). FTLE/FSLE 'ridges' are an efficient tool for identifying LCSs. In fact, there are LCSs in any dynamically active area which do not match strong ocean fronts. As an example, compare please the upper right corner on the FTLE map in Fig. 3a and on the origin map in Fig. 3b. Lagrangian fronts, in difference from LCSs, rather abstract geometric objects of an associated dynamical system, are frontal features of real physical quantities that can be measured and detected. Another advantage of Lagrangian indicators over Lyapunov exponents in identifying fronts is that the appropriately chosen indicators are able to identify not only strong fronts but passive fronts as well.

3. Fisheries at Lagrangian fronts

3.1. Pacific saury (Cololabis saira) fisheries in the northwestern Pacific Ocean

The Kuroshio-Oyashio transition zone in the northwestern Pacific is known as one of the richest fishery areas in the world due to the large nutrient content in the Oyashio waters (e.g., Sakurai, 2007). This zone is a region where different water masses converge (e.g., Qiu, 2002; Yasuda, 2003; Nishikawa et al., 2021). Flowing southwest from Subarctics, the Oyashio current converges with transformed subtropical water of the Soya Warm current near Hokkaido Island (see Fig. 2) and subtropical water originating from the Kuroshio current. This transition zone is a region with increased eddy activity with a large number of eddies of different size, lifespan and polarity.

One of the most commercially important species in this region is Pacific saury, migrating in schools from south towards the central Kuril Islands, where the fishery begins in early August. Then the schools migrate back south to Japanese islands, where the fishing season ends in late November. The feeding sites of saury and hence the rich catches were connected until recently with positions of the Oyashio branches (Uda, 1938; Fukushima, 1979; Yasuda and Watanabe, 1994; Tseng et al., 2014; Kuroda and Yokouchi, 2017) and location of the mesoscale quasi-stationary anticyclonic eddies (Saitoh et al., 1986; Sugimoto and Tameishi, 1992; Samko et al., 2007; Prants et al., 2012, 2014 and 2021). Russian and Japanese fishermen use SST images (Filatov et al., 2011; Kuroda and Yokouchi, 2017) to search for potential feeding grounds which, however, are not available in cloudy and rainy days often occurring in this region in the fishing season.

Historical catches of the Pacific saury have fluctuated over time with a significant decrease after 2014 (www.npfc.int/ summary-footprint-pacific-saury-fisheries; Hsu et al., 2021; Prants et al., 2021). Because of its commercial importance, factors influencing the abundance and distribution of Pacific saury are of considerable scientific and

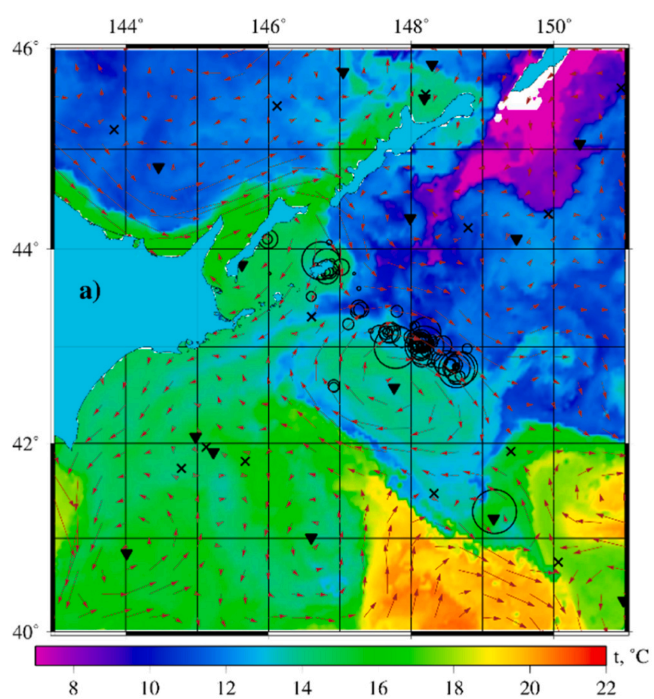

Fig. 2. SST image and the altimetric velocity field (arrows) on 17 October 2004 with the superimposed sites of maximum saury catches on that date (black circles) in the Pacific Ocean to the east off Hokkaido and southern Kuril islands. Black triangles and crosses are locations of elliptic and hyperbolic points on that date.

commercial interest. Using a database with saury catch locations in 2004 – 2019 fishing seasons, Prants et al. (2021) and Kulik et al. (2021) have found statistically significant correlation of LF locations with saury catch sites in the region. Based on the simulation results, they have been able to distinguished strong and permanent LFs with accumulation of catches associated with the Soya Warm current, the Oyashio branches and with the Hokkaido and Bussol quasi-stationary anticyclones. The proximity of catch sites to locations of the strong LFs has been shown statistically using maximum gradients of the values of the relevant Lagrangian indicators as indicators of the front locations (see Section 2).

To compare the possibilities of SST and Lagrangian diagnostics in detecting ocean fronts, we show in Figs. 2 and 3 SST image, the altimetry-based FTLE map (Fig. 3a) and origin map (Fig. 3b). The Hokkaido mesoscale quasi-stationary anticyclone appears every year in the area of confluence of the Oyashio and Soya Warm currents (Prants et al., 2014 and 2018). The origin of water masses, converging at strong fronts, can be tracked by computing the origin maps (see Section 2). Trajectories of artificial particles, distributed over the whole region shown in Fig. 3, were daily integrated backward in time to record which geographical border each particle crossed for half a year prior to the date indicated on the map. The origin map in Fig. 3b shows by yellow color the particles which entered the region through its western boundary. The green, blue and red particles entered the region through its eastern, northern and southern boundaries for half a year in the past, respectively. The boundaries between waters of different color in Fig. 3b show the locations of strong and permanent LFs. The SST image in Fig. 2 demonstrates the thermal front between subarctic and subtropical waters along the northern periphery of the Hokkaido quasi-stationary eddy. Locations of some LFs coincide with the locations of SST fronts that are visible on satellite images, although many smaller-scale features do not appear in SST images. The origin map gives much more detailed pattern of the fronts around the eddy.

It seems from the definitions that there exists nothing common between the indicator of water origin and the FTLE (Λ-map in Fig. 3a computed for two weeks in the past). However, comparing panels a) and b) in Fig. 3, it is obvious that both the maps show the same strong and persistent LFs in the area: the Soya front (S), the first (1st O) and second Oyashio (2nd O) fronts. The prominent features of the FTLE field in Fig. 3a are black 'ridges' with maximum Λ-values which approximate locations of unstable manifolds of hyperbolic objects in the region existed during, at least, the computation time of two weeks (see Fig. 1). However, there are a number of other 'ridges' which locations do not correspond to strong fronts with converging water masses of different origin. Therefore, the chances to catch saury there are small.

Inspecting the maps in Fig. 3a and b, we may conclude only that the majority of catch sites are located in the area of confluence of the Soya Warm current with the 1st and 2nd Oyashio branches. To estimate whether the saury catch sites tend to be located nearby the 'ridges' with the maximum (local) FTLE values, approximating locations of strong LFs, Prants et al. (2021) used statistical tests. The total catch by the Russian vessels until 2017 was obtained from the FAO report (Capture Production 1950–2017, www.fao.org/fishery/statistics/software/fishstatj/en). In 2018 – 2019, the data were obtained from the Russian national report to the North Pacific Fisheries Commission (Kulik et al., 2020a) available at www.npfc.int/summary-footprint-pacific-sauryfisheries.

In every fishing season, Prants et al. (2021) computed the distributions of the mean values of the FTLE gradient $\nabla\Lambda$ within 10 km distance from saury catch sites and from the points distributed randomly and repeated in 1000 trials. The empirical cumulative distribution functions were calculated for each random trial and trials with saury catches to make Fig. 4 with distributions averaged in 2004 – 2019 fishing seasons. The D-statistics from the two-sample Kolmogorov–Smirnov test were estimated between the samples with catches and samples from random distributions with the same number of points. The values of the absolute maximum distance between the two distribution functions were found

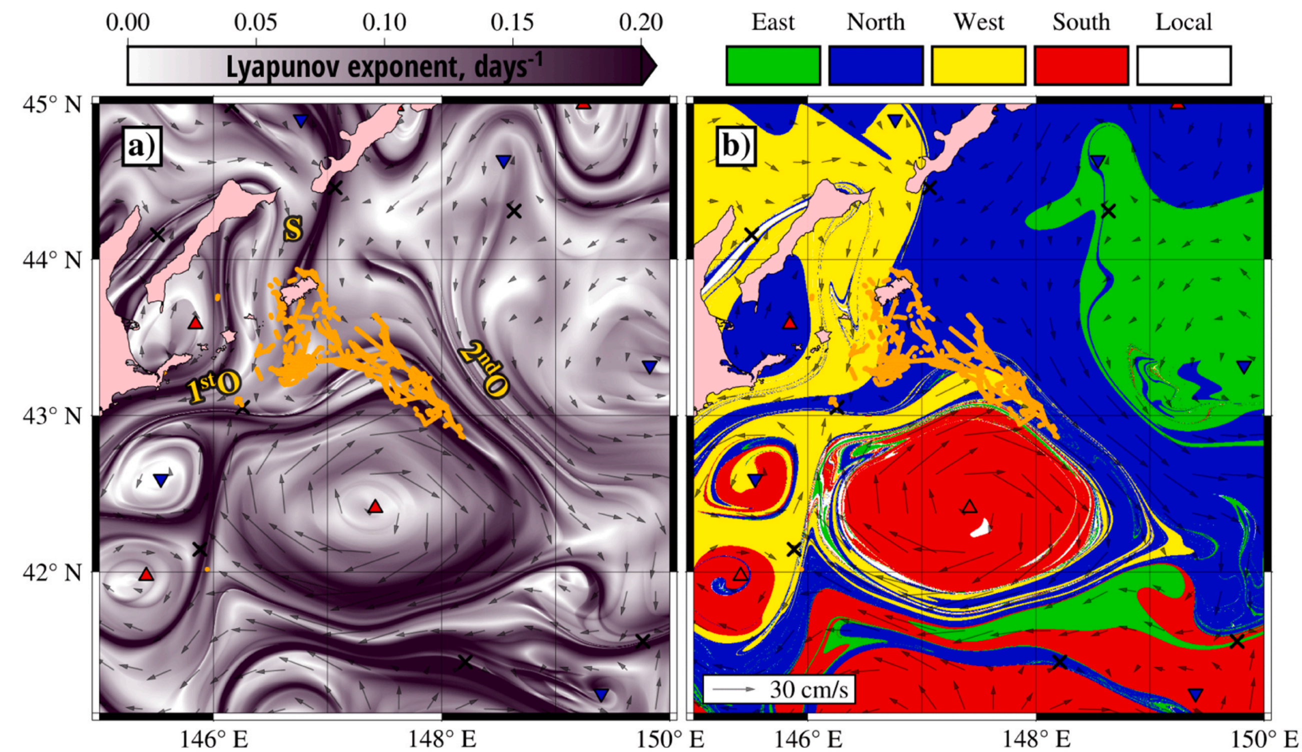

Fig. 3. a) The altimetry-based FTLE and b) origin maps on Oct. 1, 2004 around the Hokkaido quasi-stationary anticyclone centered at 42.5° N and 147.4° E with the overlaid catch sites from Sep. 24 to Oct. 8 shown by orange. S, 1st O and 2nd O are acronyms for the Lagrangian fronts associated with the Soya Warm current and the 1st and 2nd Oyashio branches. The upward-oriented (red) and downward-oriented (blue) triangles are the elliptic points corresponding to locations of the centers of anticyclones and cyclones on Oct. 1, and crosses are locations of the hyperbolic points. The grades of color in (a) modulate the values of Λ in days^{-1} .The meaning of colors in (b) is explained in the main text.

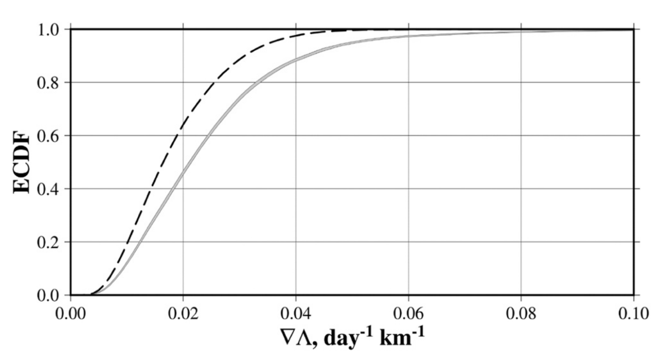

Fig. 4. Cumulative distribution functions of the mean gradient of FTLE, $\nabla\Lambda$, in a 10 km buffer from the saury catch sites (dashed curve) and randomly distributed sites. The functions were averaged over 2004 – 2019 fishing seasons (reproduced with permission from Prants et. al., 2021).

to be in the range $D = 0.175$ –0.191. All those D values have $p < 0.001$ with the median value $D = 0.184$. The Kolmogorov–Smirnov sample test shows that the catch and random distributions differ significantly starting from the value of $\nabla\Lambda \approx 0.01$ (day $\times$ km)$^{-1}$ corresponding roughly to $\Lambda > 0.1$ days^{-1} that was estimated by Prants et al. (2021) to be a threshold value approximating location of strong LFs in the study area.

The analysis of distributions of saury catch sites by Russian, Japanese and Korean vessels with the large database of fishing in the exclusive economic zone of Russia in 2004 – 2019 confirmed the correlation of the catch sites with locations of the mesoscale LFs (Prants et al., 2021). The positive effects on the encounter probability of saury were found for the FTLE gradient, while the effect of particle path length L was negative (Kulik et al., 2022). That means that saury preferred places close to LFs, but not inside eddies, where the FTLE gradients are small. The catch sites have been really found by many authors to accumulate at the edges of mesoscale eddies, but not within the vortex cores (e.g., Saitoh et al., 1986; Samko et al., 2007; Prants et al., 2014 and 2021; Kulik et al., 2022). The altimetry-based 2D Lagrangian diagnostics do not provide us with a biological/ecological explanation of that. The hydrological surveys, conducted for many years in the saury foraging area, have shown that the conditions favorable for saury feeding occur at the fronts with the seasonal pycnocline and accumulation of phytoplankton in the upper mixed layer (e.g., Filatov et al., 2011) attracting food for saury, zooplankton. The thinner the upper mixed layer, where the saury feed, the more zooplankton concentration, whereas in the absence of strong stratification, phytoplankton, food for zooplankton, is distributed homogeneously over the depth without concentrating in the subsurface layer. Hydrological conditions favorable for saury feeding are naturally met on strong and permanent LFs, in particular, at the eddy's edges (see Fig. 3 and also Schmid et al., 2020). The monthly mean of catch probability in September had the highest correlation with the Russian annual catches outside the national waters between Russia and Japan ($r = 0.76$, $p = 0.001$) and total annual catches there ($r = 0.73, p = 0.002$).

A new model for estimation of daily probability for the Pacific saury encounter was proposed by Kulik et al. (2022) motivated by the evidence of the significant decrease in saury catches after 2014 and a shift of the catch sites from traditional fishing areas near the coast of the Kuril and Japan islands east, into the open ocean (www.npfc.int/summary-footprint-pacific-saury-fisheries; Hsu et al., 2021; Prants et al., 2021). The analysis of the Empirical Orthogonal Functions (EOF) for the average daily probability of saury catches has shown that the first three variances associated with the EOF sum to 82.6 % (Kulik et al., 2022). While the first and the second EOFs were correlated with catches, the third EOF was highly correlated with published estimates of biomass of saury by Hashimoto et al. (2020). Those estimates were obtained using different methods for stratification, but the results were highly correlated ($r \geq 0.99$).

The third EOF had the remarkably similar dynamics of biomass especially from August to September ($r \geq 0.8, p < 0.05$). These results can be interpreted as an increased probability of saury catches in the open ocean (EOF3) and a significant deterioration for the catches in traditional fishing areas (EOF1 and EOF2). This conclusion has been fully confirmed by further research (see reports of the North Pacific Fisheries Commission, https://www.npfc. int/science/gis/catch-effort/saury). The developed model seems to be useful to manage fishery in the study area and may help to explain the reasons for the saury biomass decline. The latter is very important to take into account for development of the stock assessment models.

3.2. Walleye pollock (Gadus chalcogrammus) fisheries in the Sea of Okhotsk

The eastern part of the Okhotsk Sea is one of the most productive fishing areas in the northwestern Pacific providing the maximum annual catches among commercially important species. This sea is separated from the open ocean by the chain of the Kuril Islands with narrow straits. Strong tidal currents and vigorous vertical mixing occur in the straits (Nakamura et al., 2006) leading to the transfer of a significant amount of mineral forms of the main biogenic elements to the surface layers. The relatively warm and nutrient-rich ocean waters enter the sea primarily through the northern Kuril straits (Nakamura et al., 2006; Ohshima et al., 2010; Prants et al., 2015; Fayman et al., 2021) and spread northward along the western coast of Kamchatka. These waters are characterized by the maximum concentration of phytoplankton in the Okhotsk Sea (on average 500 – 1000 mg/m^3 and in some places more than 1000 mg/m^3), zooplankton and benthos (Markina and Chernyavskii, 1984). In the 21st century, the pollock commercial stock has remained approximately at the same high level and, according to estimates made using modern fishery mathematical models with survey results as input data, it ranged from 5.7 to 6.0 Mt (Kulik et al., 2020b). In the West Kamchatka and Kamchatka-Kuril fisheries subzones (see Fig. 1 in the paper by Budyansky et al., 2022), the fishing season lasts from January 1 to March 31.

The distribution of the ocean water within the Okhotsk Sea can affect the distribution of commercial fish not only through food chains, but also directly. To evaluate the statistical significance of the influence of the dynamical features on the formation of the commercial concentration of walleye pollock, Budyansky et al. (2022) tracked the origin of water in the fishery area using the Lagrangian diagnostics. They also compared the distribution of pollock catch sites with the residence time of ocean water in these places. Based on altimetry data on the speed of geostrophic currents for each day from January 31, 1997 to March 10, 2021, the trajectories of 114,000 passive particles, regularly distributed over a grid in the Okhotsk Sea, were calculated. All particles that entered the sea from the open ocean were identified, their residence time inside the sea and the straits, where they entered the sea, were determined. Using daily data on the positions of the fishing boats in 1997–2021, the Lagrangian maps of the origin and the residence time of the ocean water for this period and statistical analysis, it has been shown that the catch sites were more often located in the waters of Pacific origin that passed through the northern Kuril straits no more than 100 days before the

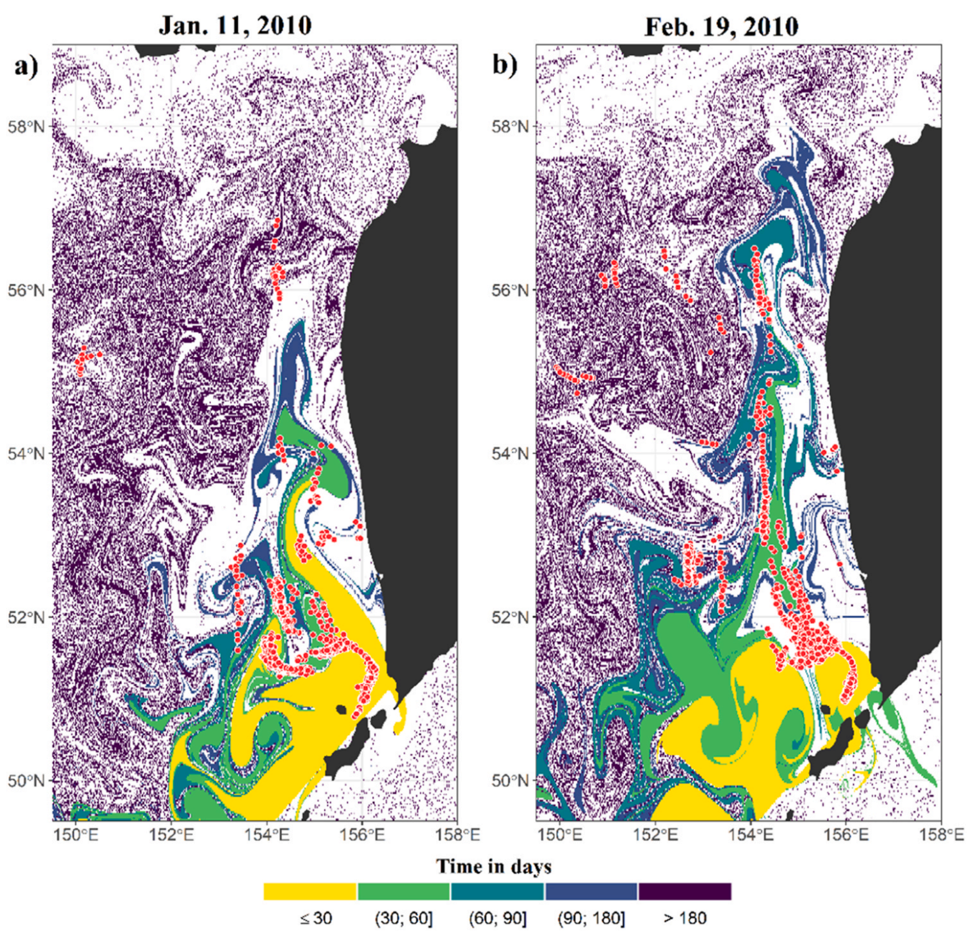

Fig. 5. Lagrangian maps show penetration of Pacific Ocean water into the eastern part of the Okhotsk Sea in the 2010 fishing season. The color modulates the residence time of the ocean water (in days) inside the sea. Red dots are positions of vessels for 3 days before and 3 days after the dates indicated on the maps. Kamchatka peninsula is shown in black.

dates of catches than in the waters with shorter residence time of 100 days that entered the Okhotsk Sea through the central and southern straits (Budyansky et al., 2022). Using statistical methods, generalized additive models (GAMs) and analysis of satellite images of SST and chl-a, they have found aggregation of pollock catch sites inside the intrusions of ocean water and on the passive LFs, as being warmer and richer in food.

The Lagrangian maps in Fig. 5 illustrate penetration of the ocean water into the eastern part of the Okhotsk Sea. As a rule, fishing in January is concentrated on the boundaries or inside 'tongues' of this water which entered the sea through the northern Kuril straits in December of the previous year or in January and advected by the West Kamchatka Current (Fig. 5a). In February, this relatively 'young' ocean water spreads northward along the western coast of Kamchatka, and catch sites are distributed throughout the West Kamchatka Current area (Fig. 5b). At the end of the fishing season, catch sites shift northwestward (not shown). The walleye pollock catch sites are concentrated primarily on relatively 'young' waters that entered the sea less than 100 days before the dates of catches.

In order to statistically test this observation, Budyansky et al. (2022) calculated the probabilities for the travel time of particles, distributed over the transect along all the Kuril Straits (see Fig. 1 in the referred paper), to randomly selected sites within the study area and to walleye pollock catch sites. Fig. 6a shows a comparison of the probability distributions of the travel time between the sites with real and false catches in 1997 – 2021.

The similar analysis was performed for the latitude at which the particles of the ocean origin crossed the transect and enter the Okhotsk Sea. The comparison of the probability distributions for the latitude of crossing among particles from randomly selected sites and those particles in the grid cells, where pollock was subsequently caught, is shown in Fig. 6b for different years. Sites with the pollock catches were located in the waters that entered the sea primarily through the Kuril straits to north of 48° N (Fig. 6b). The similar year-to-year comparison led the authors to the conclusion that the distribution of catches in those years, when the total catch was at a high level, was primarily in the relatively 'young' Pacific water that crossed the conventional Kuril transect via the northern Kuril straits. To quantify the differences between the obtained samples, the Kolmogorov-Smirnov test was performed. For the time of water travel from the transect to the cells with real and false catches, the Kolmogorov - Smirnov parameter turned out to be $D = 0.2555$ at the significance level of $p < 2.2 \cdot 10^{-16}$. For the latitude of the intersection, it was $D = 0.60818$ with $p < 2.2 \cdot 10^{-16}$. Thus, the statistical significance of the differences in both the cases turned out to be less than the machine zero (Budyansky et al., 2022).

The estimate of the cumulative effect of the considered Lagrangian indicators on the probability of pollock catch was made using the GAM with the tensor product. Among all the tested GAMs, starting from the null model and ending with the full model, the maximum proportion of dispersion (49.2 %) was described by the GAM, that included as terms the function of the ordinal number of the day in the year and the coordinates of the intersection of the conditional transect by Lagrangian particles in the cells where the catches were observed. All the used Lagrangian indicators were at the highest level of significance with $p < 0.001$. Simpler GAM configurations had higher information criteria, therefore, the resulting model may be considered as optimal.

The boundaries of the intrusions of the ocean water can be considered as passive LFs separating waters with different properties (temperature, salinity, nutrients, phyto- and zooplankton concentration) at which, however, large density gradients and submesoscale ageostrophic circulation processes are practically absent (Lévy et al., 2018). Walleye pollock catches are observed both at the boundaries of such intrusions and inside them. The role of passive LFs is that they are predictors of the presence of feed for walleye pollock. Budyansky et al. (2022) indicated that possibly walleye pollock adults are somehow able to recognize potentially favorable feeding conditions for larvae in advance. This evolutionary adaptation may be a consequence of the higher survival rate of pollock larvae in ocean water, that has higher temperature than local water of the Okhotsk Sea. The inflowing ocean water brings fish eggs to those areas where in the very near future the ice will break up, and spring phytoplankton blooms will begin providing food for the larvae. The horizontal temperature gradients may serve as an indicator in the choice of spawning grounds. In order to test this hypothesis, Budyansky et al. (2022) compared the walleye pollock catch sites with averaged SST data in the winter fishing seasons for a number of years. The walleye pollock fishing grounds in the Kamchatka–Kuril and West Kamchatka subzones (see Fig. 1 in the referred paper) have been found primarily on the boundaries of the intrusions of warm ocean water (Fig. 7).

3.3. Connection of catch locations of other species with Lagrangian fronts

The feeding grounds of neon flying squid (*Ommastrephes bartramii*) are located in the same area as saury catches (Novikov et al., 2007; Fan et al., 2009; Chen et al., 2014; Alabia et al., 2015, Li et al., 2023). Every year from June to August squid migrates north for feeding. In September, feeding occurs in the Kuroshio – Oyashio transition zone. With intensification of the Oyashio current in October–November, the schools migrate south (Novikov et al., 2007; Fan et al., 2009; Chen et al., 2014; Alabia et al., 2015). The altimetry-based Lagrangian origin maps have been used by Budyansky et al. (2017) to detect the LF locations in this area. The majority of squid catch sites has been found to be located

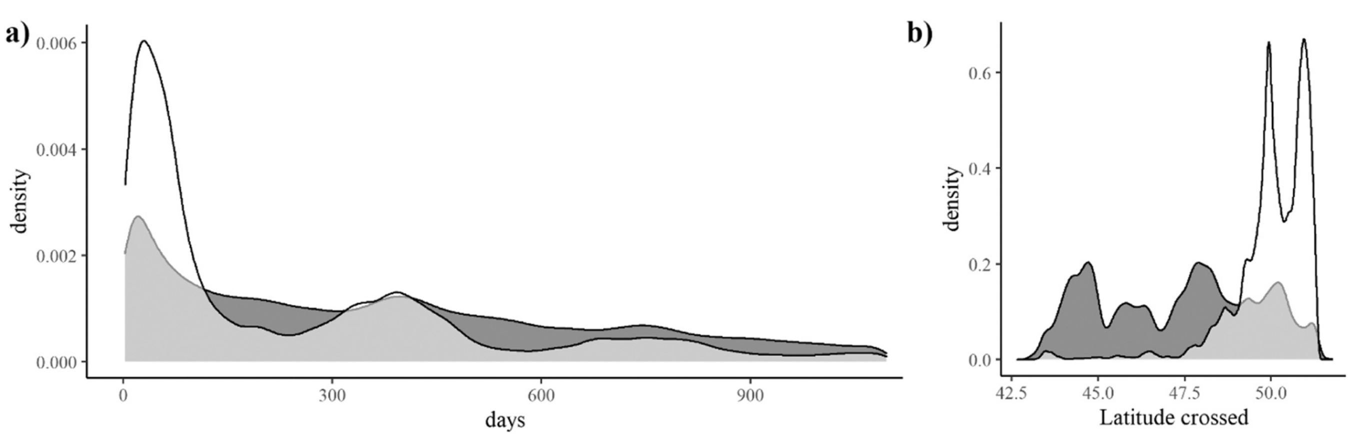

Fig. 6. a) Probability distributions for the particle's travel time from the Kuril transect to randomly chosen sites (dark line) and to the walleye pollock catch sites (light line) in 1997 – 2021. b) Probability distributions of the latitude at which particles from randomly chosen sites (dark) and from the sites where walleye pollock were subsequently caught (light) crossed the Kuril transect (adapted from Budyansky et al., 2022 with permission).

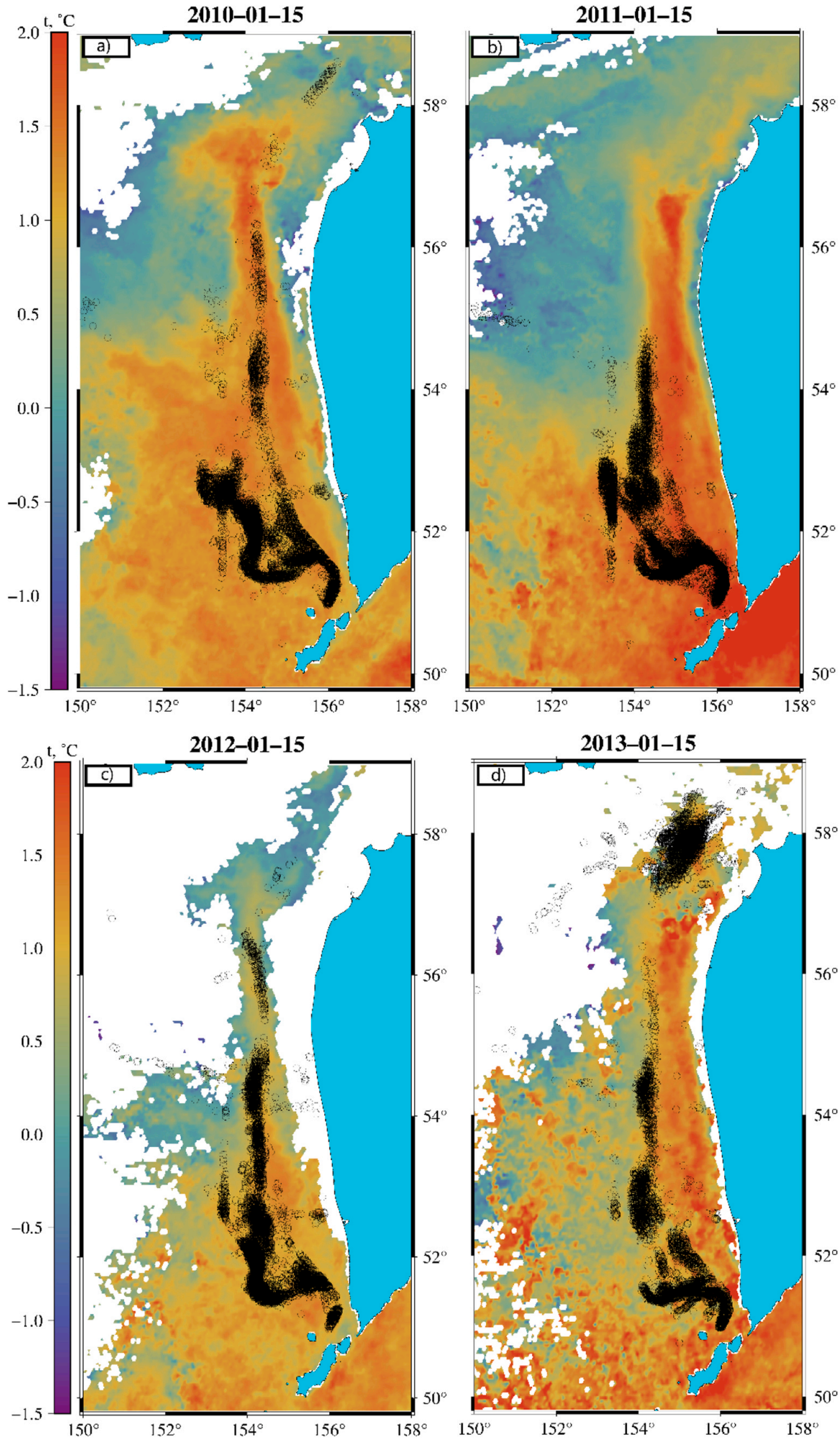

Fig. 7. Surface temperature in the eastern Okhotsk Sea during 2010 – 2013 winter fishing seasons averaged over 30 days before and after January 15 of each year with superimposed walleye pollock catches sites (black dots) over the same 60 days. SST data (MODIS) show warmer Pacific Ocean water entering the sea through the northern Kuril Straits.

on the boundaries or inside mesoscale anticyclonic eddies and along the Subarctic Front between transformed subtropical and subarctic waters (Budyansky et al., 2017; Li et al., 2023).

3.4. *The role of Lagrangian fronts in fisheries and larvae transport in California Current System and Mediterranean Sea*

Eastern boundary currents, such as the California current, are also the areas with productive fisheries, and the coastal waters there are important habitats and spawning grounds for many species of fish and invertebrates (e.g., Chassot et al., 2010). This current transports nutrient rich water from the Alaska current south along the western coast of North America. The elevated rate of productivity in this area is due to coastal upwelling, driving primary productivity. Coastal upwelling also generates mesoscale dynamic structures such as fronts and eddies. These structures organize transport of upwelled water, containing biologically important material such as nutrients, plankton and marine propagules (larvae, eggs and spores).

The relationship between fronts and fishing grounds has been studied in this area by Watson et al. (2018) using the ROMS model (Shchepetkin and McWilliams, 2005). To understand whether fishermen track FTLE 'ridges', Watson et al. (2018) compiled data on the location of over 1,000 fishing vessels every hour in the California Current System for the period 2009 – 2013 produced from the US Vessel Monitoring System. The authors modeled currents in the near surface layer with the horizontal resolution of 10 km. They focused on the spatial dynamics of vessels operating with commercially important species: the albacore tuna, chinook and coho salmon (*Oncorhynchus tshawytscha* and *Oncorhynchus kisutch,* respectively) and pink shrimp (*Pandalus jordani*). The catch sites of these species were superimposed on the FTLE maps. Statistical processing of the obtained results showed that the catches of tuna near the LFs were 3 times higher than in other places. The Kolmogorov-Smirnov p-values, indicating the significance of the difference between the sites with catches and randomly distributed sites, have been estimated to be $4 \bullet 10^{-13}$ for tune, $2 \bullet 10^{-6}$ for salmon and 0.3 for shrimp (see Fig. 2 in the referred paper), i.e., only the shrimp fishery FTLE distribution was not significantly different from random.

Incidental catch of nontarget species (bycatch) poses a threat to the populations of sharks, dolphins, sea turtles, seals, seabirds and other species. That is a major barrier to ecological and economic sustainability in marine fisheries. It has been shown by Scales et al. (2018) that the Lagrangian analysis can help in the estimate of the likelihood of marine megafauna bycatch in the dynamic ocean environments which transport water masses and affect their properties on a large range of temporal scales, including those of ecological relevance. Scales et al. (2018) used the high-resolution ROMS model output to identify FTLE 'ridges' in the California Current System to assess the risk of incidental catches. A statistical analysis of the catch sites for various fish species in 1990 – 2010 for 1,357 voyages of fishing vessels showed that incidental catches were significantly more likely at the LFs identified by the FTLE 'ridges'. These results highlight how the real-time tracking of dynamic structures can support fisheries sustainability and advance ecosystem-based management. For example, the observed functional responses of tunas to submesoscale thermal fronts established that teleost fish were likely to be closer to the surface when exploiting forage resources on the warm side of a front, and deeper when targeting forage resources on the cold side (Snyder et. al., 2017). This suggests that a strategy, targeting surface aggregations on the warm side of a convergent front, could avoid interactions with other nontarget predators exploiting the same bait fish aggregation near the thermocline beneath the cooler side of the front (Scales et al., 2018).

The frontal features can aggregate larvae from many source regions into small, highly dense packets where the density can be up to two orders of magnitude greater then initial densities near the coast (e.g., Harrison et al., 2013). Harrison et al. (2013) used the modeling framework, consisting of the circulation model ROMS and a particle-tracking model, to keep track of simulated larvae and FTLE as a diagnostic for the location of strong LFs. To test the relationship between the locations of the LFs and SST fronts, these authors checked if a Lagrangian particle is on a FTLE 'ridge', than how much more likely it is on a SST front. Comparing distributions of the FTLE 'ridges', larvie density, SST and near-surface vertical velocity, they have found that larvae were primarily located on the LFs and SST fronts with enhanced vertical velocities on either side of the front (see Fig. 2 in Harrison et al., 2013).

Fig. 5c in the refereed paper compares the complementary cumulative distribution of the SST gradient magnitude with the distribution at all particle positions and for particles near the LFs with FTLE $>$ 0.2 day^{-1}. The particles were more likely to be on higher values of the SST gradient than if randomly distributed, while particles on or near the LFs were even more likely to be on high SST gradient values (50–60 % above 0.1 $^\circ$C $\times$ km^{-1}, twice as many as expected; $p < 0.001$ for all comparisons). This demonstrates that larvae were more likely to be on LFs (see Fig. 1 for evolution of a tracer patch). This study has shown that the frontal structures play an important role in pelagic transport of marine larvae.

Russo et al. (2022) used the Lagrangian simulation approach in order to investigate the fate of the tuna larval stages and their relation with environmental conditions in the central Mediterranean Sea. The technique, based on calculation of larval backward trajectories, allowed them to estimate the larval pathway and to identify the spawning areas. The authors analyzed tuna larvae that originated from multiple spawning events and found that, regardless of the spawning area, the larvae released into the area ended up concentrating in a common retention area related to a local frontal mesoscale oceanographic feature. Generally, tuna larvae are trapped by the thermohaline front and by the local mesoscale circulation, which favor concentration processes. The Lagrangian approach can provide useful information to support tuna fisheries management. Better information on spawning areas and larval habitats can help establish marine protected areas or areas closed to fishing.

Using ichthyoplankton samples collected over four years, Díaz-Barroso et al. (2022) have examined how sea surface mixing activity, parameterized by satellite-derived FSLE, provided information on the environmental conditions that defined Atlantic bluefin (*Thunnus thynnus*) larval habitats in the Western Mediterranean. The main aim was to find the spatial scales at which the relationship between FSLE and the probability of presence of larvae emerged. It has been found that the presence of bluefin tuna larvae was not correlated with the front locations, i.e., with high FSLE values, but was correlated with areas with low/moderate FSLE values of the order of 0.1 day^{-1}. It means that strong turbulence (mixing), at least in the study area, has a negative effect on larvae by disaggregating food and larvae patches and on recruitment. Following to the optimal environmental window hypothesis (Cury and Roy, 1989), the fitness of early life stages is maximized at intermediate values of mixing activity due to an interplay between physical and biological constraints (food availability and predator presence).

Manso-Narvarte et al. (2023) have studied the influence of eddies, fronts and along-slope currents on the distribution of eggs and larvae of European anchovy (*Engraulis encrasicolus*) in the Bay of Biscay (Atlantic Ocean) by performing the FSLE diagnostic based on high-frequency radar data. The resulting transport patterns have been shown to be caused by a combination of eddies, fronts and along-slope currents. These features were identified as the mesoscale structures that can shape the distribution of the larvae. Eddies were able to trap fish larvae, whereas the fronts served as transport barriers between coastal and offshore waters.

Effects of eddies on the distribution and food availability of larvae of different species have been studied with the help of *in situ* measurements in different regions (e.g., Hare and Cowen, 1996; Logerwell and Smith, 2001; Kasai et al., 2002; Okazaki et al., 2002; Govoni et al., 2010; Shulzitski et al., 2015 and 2016; Suthers et al., 2023).

3.5. In situ measurements of fish concentration at Lagrangian fronts

Baudena et al. (2021) have conducted a study in the Indian sector of the Southern Ocean by comparing acoustic measurements of mesopelagic fish (myctophids) concentrations with the satellite-derived fine-scale LFs. The functioning of this subantarctic area is primarily regulated by the Kerguelen plateau that is a major topographic barrier for the Antarctic Circumpolar Current. The plateau fertilizes in iron, a limiting nutrient, the waters advected by this current. Depending on seasonal light conditions and stratification of the water column, this provokes a large annual phytoplankton bloom which supports a rich trophic web. This is one of the reasons for which the Kerguelen archipelago and surrounding waters are part of one of the ten largest marine protected areas in the world (http://www.mpatlas.org). Myctophids are one of the most abundant groups of mesopelagic fish in the oceans and are thought to constitute one of the largest portions of the world fish biomass (Irigoien et al., 2014). They also represent important prey for numerous predators (Cherel et al., 2010).

Baudena et al. (2021) used FSLE (see Section 2) and SST gradient as diagnostics to detect frontal features, since they are typically associated with the LF locations (Prants et al., 2014; Lehahn et al., 2018). The LFs may display enhanced SST gradients because water masses of different origin have often contrasted SST signature. However, this is not a necessary condition. The LFs, including the Lyapunov 'ridges', may be invisible in SST maps if transport occurs in a region of almost homogeneous SST. Conversely, SST gradient unveils structures separating waters of different temperatures, whose contrast is often, but not always, associated with horizontal transport. Therefore, even if they usually detect the same structures, these two metrics are complementary. Frontal features were detected by Baudena et al. (2021) considering local FSLE and SST gradient values larger than a given threshold. The threshold value has been chosen heuristically to be $\Lambda = 0.08$ day^{-1} that is close to the one found in other regions (Tew Kai et al., 2009; Watson et al., 2018; Prants et al., 2021).

The acoustic fish concentration, co-located with the FSLE and SST gradient values over the threshold, were considered as measured in proximity of the LFs (i.e., statistically associated with LFs), while the fish concentration values below the threshold were considered as not associated with the frontal structures. The bootstrap analysis was applied to estimate the probability that the difference in the mean acoustic fish concentration values, over and under the threshold, was significant, and not the result of statistical fluctuations. The other factors such as prey or predator distributions may influence the fish distribution other than the frontal activity considered. The presence of these factors can shadow the relationship of the explanatory variables (FSLE values and the SST gradient) with the mean value of the response variable (the acoustic fish concentration). Linear quantile regression method was employed to address this problem.

The higher fish concentrations have been found to occur more frequently in correspondence with the strong LF (Fig. 8) with the significance of the bootstrap test $p < 0.001$. While the increased fish densities were more likely to be observed over the LFs, the presence of a fine-scale feature does not imply a concomitant fish accumulation, as other factors affect fish distribution. Finally, when only chl-a-rich waters were considered, front intensity modulates significantly more than the local fish concentration (Baudena et. al., 2021).

4. Discussion

The plankton, that is the basis of the food chain in the ocean, follows evolving LFs (see Fig. 1) and develops into complex patterns with lobes, filaments and swirls formed as a result of (sub)mesoscale advection (see e.g., Abraham, 1998; Martin, 2003; Martin et al., 2002; Lehahn et al., 2007 and 2018; d'Ovidio et al., 2010 and 2013). The vertical motion at strong and permanent fronts due to submesoscale ageostrophic processes delivers nutrients to the depleted euphotic layer and promotes growth and accumulation of phyto- and zooplankton. These physical processes contribute to biological activity at all levels of the food chain, from phyto- and zooplankton to small and large pelagic fish, seabirds and top predators.

Clayton et al. (2014) and De Verneil et al. (2019) have studied the phytoplankton community structure across fronts. They observed increased chl-a content along inclined isopycnals across the Kuroshio Front and at the front off the coast of California, respectively. Phytoplankton biomass was elevated, where there was a positive vertical flux of nitrate towards the surface, and the local circulation drove a lateral transport of nutrients to the front. The physical forcing at strong fronts drives small-scale motions that perturb the biological system more rapidly than either acclimation or resource uptake can respond leading to the appearance of un-acclimated populations at the fronts.

Bertrand et al. (2014) collected high-resolution and wide-range acoustic and GPS-tracking data in the Northern Humboldt Current

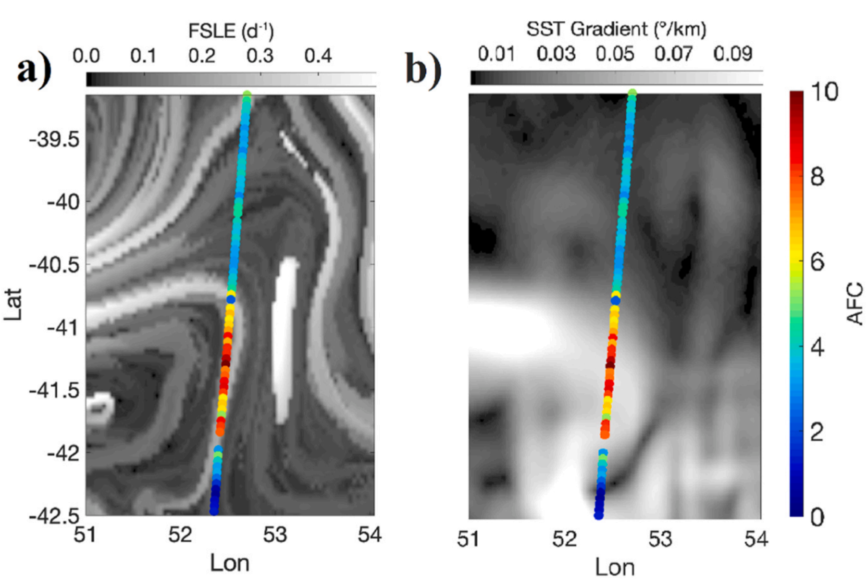

Fig. 8. a) Illustrative example of a transect of the ship trajectory on August 29, 2014, superimposed on the simultaneous FSLE field with the white bands corresponding to the maximum FSLE values. The color of each dot is proportional to the local acoustic fish concentration (AFC, nondimensional, scale at right). b) Same as for panel a) with the difference that the transect is superimposed on the simultaneous SST gradient (from Baudena et. al., 2021 with permission).

System off Peru, one of the most productive fishery area. They have shown that the ecosystem interactions may occur not only at strong permanent fronts at meso- or submesoscale but within small, short-lived fronts and small coherent eddies that create small-scale, O (1–4) km, ephemeral hotspots, where a variety of organisms, ranging from zooplankton to pelagic fish and seabirds, may concentrate.

Fronts are known to play an essential role in partitioning phytoplankton assemblages (e.g., Olson et al., 1994; Lehahn et al., 2007 and 2018; d'Ovidio et al., 2010; Scales et al., 2014; Lévy et al., 2018; Hernández-Carrasco et al., 2020; Mangolte et al., 2023; Ito et al., 2023). Liu et al. (2018) have examined the correlation between permanent mesoscale fronts and the spatial distribution of some microfossils at the sea floor. Ten major fronts and four primary microfossil assemblages in the Bohai, Yellow and East China seas were identified. Analyses of the spatial patterns of fronts, microfossil assemblages, SST, salinity and nutrients revealed that the fronts partitioned the microfossils deposited at the sea floor into the assemblage types corresponding to the physicochemical features of the frontal water masses.

As it was noted in Introduction, *in situ* location of ocean fronts is practically impossible on a global scale. Lagrangian indicators and LFs, associated with the presence of strong environmental gradients, provide us with complementary (to SST and chl-a data) information regarding flow properties: the current state of circulation, the origin and advection history of converging water masses, their 'age', retention and residence times, the location of barriers to transport, quantitative measures of chaotic water motion in the proximity of LFs (FTLE and FSLE), the distance covered by frontal particles, etc.

The spatial scale of LFs is given by the spatial resolution at which the relevant Lagrangian indicators are calculated. One of the advantages of using LFs is that they are able to reveal hydrological fronts below the nominal resolution of the velocity field. The robustness of the FTLE/FSLE diagnostics and the sensitivity of the Lyapunov 'ridges' to errors in the altimetric velocity field have been investigated by (Haller, 2011), Hernández-Carrasco et al. (2011), Keating et al. (2011) and Harrison and Glatzmaier (2012). The identified frontal features have been found to be relatively insensitive to both sparse spatial and temporal resolution and to the velocity field interpolation method. This means that through LFs we can capture some effects of the large-scale structures on scales which are smaller than the resolution of the altimetry data due to capacity of the Lagrangian diagnostics to exploit the spatiotemporal variability of the velocity field by following particle trajectories.

However, there are some limitations of the Lagrangian analysis based on the conventional altimetry data. First of all, these data have comparatively low spatial and temporal resolutions of the order of $0.25^\circ \times 0.25^\circ$ and daily time step for the global coverage and two and three times more fine resolution in some regions. The basic shortcoming of the altimetry-based Lagrangian results is in the assumption that the geostrophic velocity field is known with good accuracy, which is not always the case in practical applications. Higher spatial resolution is needed to go beyond the mesoscale and observe submesoscale features.

The launch of the SWOT mission (Surface Water and Ocean Topography) in the end of 2022 opens up new opportunities compared with the conventional altimeters due to higher resolution of SWOT, in particular, in regions with small Rossby radius and reduced noise close to the coast (Fu et., al, 2024). The SWOT altimeters enable high resolution monitoring of coastal regions within 1 km from land. SWOT observations are expected to provide a spatial resolution of 15 km at low latitudes and 30–45 km at higher latitudes allowing to resolve submesoscale features, like filaments and small-scale eddies and fronts which are not resolved by classical altimeters. Although SWOT do not measure the vertical velocities directly, but the locations of the fine-scale surface heights and currents could indicate on the places with increased upwelling that occurs at fronts, opening a new field of studies of vertical dynamics. All these advantages of high-resolution SWOT altimetry will provide us with unprecedented 'ground truth' on the role of fine-scale circulation in marine ecology and fishery. The already developed Lagrangian methods for predicting LFs with favorable fishery conditions are SWOT-ready, i.e., as soon as wide-swath SWOT global mapping data are available, these and other Lagrangian methods can be applied, and better results than those nadir-based are expected.

The second point is that any altimetry data are limited to two dimensions. Therefore, to validate

the presence of LFs with potentially favorable biophysical conditions, it is required either to carry out the measurements of concentration of plankton biomass at identified fronts as it has been done, for example, by Clayton et al. (2014), De Verneil et al. (2019), Ser-Giacomi et al. (2021) and many others or to estimate fish concentration using a sonar (e.g., Baudena et al., 2021). Both the means are problematic to widely use. The modern numerical circulation models and reanalyses with high spatial and temporal resolutions allow to simulate 3D frontal structures.

The third caveat is that invariant manifolds and associated fronts and LCSs are transport barriers for passive particles in theory. In fact, they are leaky. For fishery, it means that phyto- and zooplankton can cross fronts but it occurs, if any, over comparatively small distance away from the front that is small enough to allow prediction of locations of potential fishing grounds. As it has been shown in a number of papers (e.g., Haller, 2002 and 2015; Haza et al., 2016; Onink et al., 2019; Moral-es-Márquez et al., 2023), the LCSs computed from mesoscale surface velocity fields can be considered as a good first-order proxy, but the leakage of material across them at submesoscale can be significant.

Nutrients, plankton and debris accumulate at fronts and form clusters due to convergence. Identifying where the clusters form can aid in locating hotspots of biological activity important for fishery. To diagnose regions likely to contain clusters without the need to integrate millions of trajectories, Huntley et al. (2015) proposed a new Lagrangian metrics for defining clusters. They called this dilation, which quantifies area changes of patches with advected virtual particles. The idea is to decompose material deformation into dilation and area-preserving stretch processes to refine FTLE/FSLE-based approaches by splitting the Lyapunov exponents into fundamental kinematic properties. The application of this metric was illustrated with a data-assimilating circulation model of the Gulf of Mexico where the regions of dilation less than one have been shown to be much more likely to be visited by particles than those of dilation greater than one. A closely related metric, the Lagrangian divergence along fluid trajectories, has been proposed by Hernández-Carrasco et al. (2018) to investigate the influence of fine-scale dynamics in the range of submesoscale and low mesoscale on surface phytoplankton derived from satellite chl-a imagery. This Lagrangian metrics has been computed in the velocity field provided by high-frequency radars up to 70 km from the coast of Ibiza (Spain) with hourly temporal resolution and a 1.6 km spatial resolution. It has been shown that attracting small-scale fronts, detected by the FSLE metrics, were associated with negative divergence where particles and chl-a standing stocks cluster. Filaments of positive divergence, representing large accumulated upward vertical velocities and suggesting accrued injection of subsurface nutrients, match areas with large chl-a concentration.

Another point, that deserves a discussion, is the role of passive fronts in fisheries. Passive LFs are identified as large lateral gradients of the plankter concentration and/or of some relevant Lagrangian indicators like the residence time of 'foreign' water masses intruding into a basin with 'a domestic' water (Budyansky et al., 2022). Phytoplankton can grow at passive fronts with a translation to higher trophic levels including apex predators (d'Ovidio et al., 2010, 2013; Cotté et al., 2015; Della Penna et al., 2015, 2017; Lehahn et al., 2018; Lévy et al., 2018; Mangolte et al., 2023). Due to horizontal stirring by currents, a post-blooming plankton patch is advected and stretched until it forms sub- or mesoscale filaments which boundaries are passive LFs, attracting fish in search for food.

The active and passive LFs in a given velocity field are relatively easy to compute and analyze under any weather conditions. The problem is to obtain data on fishing boat locations with and without catches for a long period of time in order to perform statistical analysis and find whether fish prefer to feed at the boundaries of LFs or not. The task is further complicated because there may be favorable conditions for feeding at a specific front but either fish schools or captains of fishing vessels were not able to find these places at time. Those fronts are missed from statistical sampling.

Fish concentrate at ocean fronts, where it is enough food for feeding. Daily maps of the relevant Lagrangian indicators with indication of location of strong and permanent LFs, transmitted in almost real time aboard fishing vessels via e-mail, could help fishermen to identify potential fishing grounds, saving time and fuel to search for fish schools. This procedure is now tested with fishing vessels operating in the Far Eastern seas of Russia.

Fish, marine animals and birds are able to seek out fronts and use them as foraging routes and feeding sites in the ocean 'desert'. To mitigate the consequences of anthropogenic pressure on the oceans, in addition to imposing various kinds of restrictions, special hopes are put on the organization of marine protected areas both in exclusive economic zones and in the open ocean (Hyrenbach et al., 2000; Grantham et al., 2011; Lascelles et al., 2012; Miller and Christodoulou, 2014; Scales et al., 2014; Della Penna et al., 2017). The frontal zones, being 'dining rooms' for many sea creatures, are promising places for organization of protected areas. Among a variety of frontal zones, it is necessary to find those ones which are sufficiently strong, permanent, predictable and have a high level of bioproductivity and biodiversity. Long-term retrospective calculations of Lagrangian maps of the relevant indicators along with detection of fronts using SST and SeaWiFS ocean color imagery may provide us with a representative picture of the distribution and properties of fronts and allow for estimation of their persistence and spatio-temporal variability in order to help in making decisions on the organization of marine protected areas.

5. Summary

This overview synthesizes the studies on fisheries at Lagrangian fronts (LFs) that are proxies for locations of oceanic frontal zones. It is a novel issue that is developing rapidly during the last decade. We review the application of the Lagrangian methods of detecting potential feeding and fishing grounds and the connection of LFs with the catches of different species of pelagic fish and squid. Lagrangian maps of the relevant indicators of sea-water motion is a suitable tool to study fisheries at the LFs because they contain information not only on the current position of frontal features, but also on the origin and advection history of frontal water masses. Moreover, inspection of the subsequent maps allows one to identify different phases of the evolution of fronts including frontogenesis, frontolysis and eventual disappearance. The Lagrangian approach improves our understanding of the marine life at fronts. The proximity of catch sites of a variety of species to the locations of active and passive LFs has been demonstrated in the northwestern Pacific, Okhotsk Sea, California Current System, Mediterranean Sea and in the subantarctic area of the Southern Indian Ocean using different statistical tests and models. The further development of Lagrangian methods gives a perspective in marine ecology and sustainable fisheries. Further research is also needed to implement these metrics in modern stock assessments and management practices.

Declaration of Competing Interest

The authors declare the following financial interests/personal relationships which may be considered as potential competing interests: S. V. Prants reports financial support was provided by V.I. Il'ichev Pacific Oceanological Institute of the Russian Academy of Sciences. S.V. Prants reports a relationship with V.I. Il'ichev Pacific Oceanological Institute of the Russian Academy of Sciences that includes: funding grants. If there are other authors, they declare that they have no known competing financial interests or personal relationships that could have appeared to influence the work reported in this paper

Data Availability

Data will be made available on request.

Acknowledgments

This work was supported by the State Task No. 124022100072-5 at the Pacific Oceanological Institute. I am grateful to an anonymous reviewer for the careful reading of the manuscript and useful advices.

References

Abraham, E.R., 1998. The generation of plankton patchiness by turbulent stirring. Nature 391 (6667), 577–580. https://doi.org/10.1038/35361.

Ainley, D.G., Dugger, K.D., Ford, R.G., Pierce, S.D., et al., 2009. Association of predators and prey at frontal features in the California Current: competition, facilitation, and co-occurrence. Mar. Ecol. Prog. Ser. 389, 271–294. https://doi.org/10.3354/meps08153.

Alabia, I.D., Saitoh, S.-I., Mugo, R., Igarashi, H., et al., 2015. Seasonal potential fishing ground prediction of neon flying squid (Ommastrephes bartramii) in the western and central North Pacific. Fish. Oceanogr. 24 (2), 190–203. https://doi.org/10.1111/fog.12102.

Bakun, A., 2006. Fronts and eddies as key structures in the habitat of marine fish larvae: opportunity, adaptive response and competitive advantage. Sci. Mar. 70 (S2), 105–122. https://doi.org/10.3989/scimar.2006.70s2105.

Basson, M., 1999. The importance of environmental factors in the design of management procedures. ICES J. Mar. Sci. 56, 933–942. https://doi.org/10.1006/jmsc.1999.0541.

Baudena, A., Ser-Giacomi, E., D'Onofrio, D., Capet, X., et al., 2021. Fine-scale structures as spots of increased fish concentration in the open ocean. Sci. Rep. 11 (1), 15805 https://doi.org/10.1038/s41598-021-94368-1.

Belkin, I.M., 2021. Remote sensing of ocean fronts in marine ecology and Fisheries. Remote Sens 13 (5), 883. https://doi.org/10.3390/rs13050883.

Belkin, I.M., Hunt, G.L., Hazen, E.L., Zamon, J.E., et al., 2014. Fronts, fish, and predators (editorial). Deep Sea Res. Part II 107, 1–2. https://doi.org/10.1016/j.dsr2.2014.07.009.

Belkin, I.M., O'Reilly, J.E., 2009. An algorithm for oceanic front detection in chlorophyll and SST satellite imagery. J. Mar. Syst. 78, 319–326. https://doi.org/10.1016/j.jmarsys.2008.11.018.

Bertrand, A., et al., 2014. Broad impacts of fine-scale dynamics on seascape structure from zooplankton to seabirds. Nat. Commun. 5, 5239. https://doi.org/10.1038/ncomms6239.

Boffetta, G., Lacorata, G., Redaelli, G., Vulpiani, A., 2001. Detecting barriers to transport: a review of different techniques. Phys. D. Nonlinear Phenom. 159 (1), 58. https://doi.org/10.1016/S0167-2789(01)00330-X.

Bost, C.A., Cotté, C., Bailleul, F., Cherel, Y., et al., 2009. The importance of oceanographic fronts to marine birds and mammals of the southern oceans. J. Mar. Syst. 78 (3), 363–376. https://doi.org/10.1016/j.jmarsys.2008.11.022.

Branch, T.A., Hilborn, R., Haynie, A.C., Fay, G., Flynn, L., Griffiths, J., et al., 2006. Fleet dynamics and fishermen behavior: lessons for fisheries managers. Can. J. Fish. Aquat. Sci. 63, 1647–1668. https://doi.org/10.1139/f06-072.

Budyansky, M.V., Kulik, V.V., Kivva, K.K., Uleysky, M.Yu, Prants, S.V., 2022. Lagrangian Analysis of Pacific Waters in the Sea of Okhotsk Based on Satellite Data in Application to the Alaska Pollock Fishery. Izv., Atmos. Ocean. Phys. 58 (12), 1427–1437. https://doi.org/10.1134/S0001433822120088.

Budyansky, M.V., Prants, S.V., Samko, E.V., Uleysky, M.Y., 2017. Identification and Lagrangian analysis of oceanographic structures favorable for fishery of neon flying squid (Ommastrephes bartramii) in the South Kuril area. Oceanology 57 (5), 648–660. https://doi.org/10.1134/S0001437017050034.

Buesseler, Jayne, K.O., Fisher, S.R., Rypina, N.S., et al., 2012. Fukushima derived radionuclides in the ocean and biota off Japan. PNAS 109 (16), 5984–5988. https://doi.org/10.1073/pnas.1120794109.

Chassot, E., Bonhommeau, S., Dulvy, N.K., Mélin, F., Watson, R., Gascuel, D., Le Pape, O., 2010. Global marine primary production constrains fisheries catches. Ecol. Lett. 13, 495–505. https://doi.org/10.1111/j.1461-0248.2010.01443.x.

Chen, X., Tian, S., Guan, W., 2014. Variations of oceanic fronts and their influence on the fishing grounds of Ommastrephes bartramii in the Northwest Pacific. Acta Oceanol. Sin. 33 (4), 45–54. https://doi.org/10.1007/s13131-014-0452-3.

Cherel, Y., Fontaine, C., Richard, P., Labatc, J.-P., 2010. Isotopic niches and trophic levels of myctophid fishes and their predators in the Southern Ocean. Limnol. Oceanogr. 55 (1), 324. https://doi.org/10.4319/lo.2010.55.1.0324.

Clayton, S., Nagai, T., Follows, M.J., 2014. Fine scale phytoplankton community structure across the Kuroshio Front. J. Plankton Res. 36 (4), 1017–1030. https://doi.org/10.1093/plankt/fbu020.

Cotté, C., d'Ovidio, F., Dragon, A.-C., Guinet, C., Lévy, M., 2015. Flexible preference of southern elephant seals for distinct mesoscale features within the Antarctic Circumpolar Current. Prog. Oceanogr. 131, 46–58. https://doi.org/10.1016/j.pocean.2014.11.011.

Cury, P., Roy, C., 1989. Optimal environmental window and pelagic fish recruitment success in upwelling areas. Can. J. Fish. Aquat. Sci. 46, 670–680. https://doi.org/10.1139/f89-086.

d'Ovidio, F., De Monte, S., Alvain, S., Dandonneau, Y., Levy, M., 2010. Fluid dynamical niches of phytoplankton types. Proc. Natl. Acad. Sci. 107 (43), 18366–18370. https://doi.org/10.1073/pnas.1004620107.

d'Ovidio, F., De Monte, S., Della Penna, A., Cotté, C., Guinet, C., 2013. Ecological implications of eddy retention in the open ocean: a Lagrangian approach. J. Phys. A 46 (25), 254023. https://doi.org/10.1088/1751-8113/46/25/254023.

d'Ovidio, F., Della Penna, A., Trull, T.W., Nencioli, et al., 2015. The biogeochemical structuring role of horizontal stirring: Lagrangian perspectives on iron delivery downstream of the Kerguelen Plateau. Biogeosciences 12, 5567–5581. https://doi.org/10.5194/bg-12-5567-2015.

d'Ovidio, F., Fernandez, V., Hernandez-Garcнa, E., Lopez, C., 2004. Mixing structures in the Mediterranean Sea from finite-size Lyapunov exponents. L17203 Geophys. Res. Lett. 31 (17). https://doi.org/10.1029/2004GL020328.

De Monte, S., Cotté, C., d'Ovidio, F., Levy, M., et al., 2012. Frigatebird behaviour at the ocean-atmosphere interface: integrating animal behaviour with multi-satellite data. J. R. Soc. Interface 9, 3351–3358. https://doi.org/10.1098/rsif.2012.0509.

De Verneil, A., Franks, P.J.S., Ohman, M.D., 2019. Frontogenesis and the creation of fine-scale vertical phytoplankton structure. J. Geophys. Res. Oceans 124 (3), 1509–1523. https://doi.org/10.1029/2018jc014645.

Della Penna, A., De Monte, S., Kestenare, E., Guinet, C., d'Ovidio, F., 2015. Quasiplanktonic behavior of foraging top marine predators. Sci. Rep. 5 (1), 18063. https://doi.org/10.1038/srep18063.

Della Penna, Koubbi, A., Cotté, P., Bon, C., et al., 2017. Lagrangian analysis aof multi-satellite data in support of open ocean Marine Protected Area design. Deep Sea Res. Part II 140, 212–221. https://doi.org/10.1016/j.dsr2.2016.12.014.

Díaz-Barroso, L., Hernández-Carrasco, I., Orfila, A., Reglero, P., et al., 2022. Singularities of surface mixing activity in the Western Mediterranean influence bluefin tuna larval habitats. Mar. Ecol. Prog. Ser. 685, 69–84. https://doi.org/10.3354/meps13979.

Dunn, D.C., Boustany, A.M., Halpin, P.N., 2011. Spatio-temporal management of fisheries to reduce by-catch and increase fishing selectivity. Fish Fish 12, 110–119. https://doi.org/10.1111/j.1467-2979.2010.00388.x.

Essington, T.E., Beaudreau, A.H., Wiedenmann, J., 2006. Fishing through marine food webs. Proc. Natl. Acad. Sci. U. S. A. 103, 3171–3175. https://doi.org/10.1073/pnas.0510964103.

Fahlbusch, Czapanskiy, J.A., Calambokidis, M.F., Cade, J., et al., 2022. Blue whales increase feeding rates at fine-scale ocean features. Proc. R. Soc. B 289, 20221180. https://doi.org/10.1098/rspb.2022.1180.

Fan, W., Wu, Y., Cui, X., 2009. The study on fishing ground of neon flying squid, Ommastrephes bartrami, and ocean environment based on remote sensing data in the Northwest Pacific Ocean. Chin. J. Oceanol. Limnol. 27 (2), 408–414. https://doi.org/10.1007/s00343-009-9107-1.

Fayman, P.A., Prants, S.V., Budyansky, M.V., Uleisky, M.Yu, 2021. Simulated pathways of the Northwestern Pacific water in the Okhotsk Sea. Izv., Atmos. Ocean. Phys. 57 (3), 329–340. https://doi.org/10.1134/S000143382103004X.

Fifani, G., Baudena, A., Fakhri, M., Baaklini, G., Faugère, Y., Morrow, R., Mortier, L., d'Ovidio, F., 2021. Drifting speed of Lagrangian fronts and oil spill dispersal at the ocean surface. Remote Sens 13 (22), 4499. https://doi.org/10.3390/rs13224499.

Filatov, V.N., Startsev, A.V., Ustinova, E.I., Eremin, E.V., 2011. Pacific Saury. Scientific and Informational Support of a Fishing Expedition. Rostov-on-Don, Russia, Southern Scientific Center of RAS [in Russian].

Franks, P.J.S., 1992a. Sink or swim: Accumulation of biomass at fronts. Mar. Ecol. Prog. Ser. 82, 1–12. https://doi.org/10.3354/meps082001.

Franks, P.J.S., 1992b. Phytoplankton blooms at fronts: patterns, scales, and physical forcing mechanisms. Rev. Aquat. Sci. 6 (2), 121–137.

Fu, L.-L., Pavelsky, T., Cretaux, J.-F., Morrow, R., et al., 2024. The Surface Water and Ocean Topography Mission: A breakthrough in radar remote sensing of the ocean and land surface water. Geophys. Res. Lett. 51, e2023GL107652 https://doi.org/10.1029/2023GL107652.

Fukushima, S., 1979. Synoptic analysis of migration and fishing conditions of saury in the northwest Pacific ocean. Bull. Tohoku Reg. Fish. Res. Lab 4, 1–70.

Fulton, E.A., Smith, A.D., Smith, D.C., van Putten, I.E., 2011. Human behaviour: the key source of uncertainty in fisheries management. Fish Fish 12, 2–17. https://doi.org/10.1111/j.1467-2979.2010.00371.x.

Godø, Samuelsen, O.R., Macaulay, A., Patel, G.J., et al., 2012. Mesoscale eddies are oases for higher trophic marine life. PLoS ONE 7 (1), e30161. https://doi.org/10.1371/journal.pone.0030161.

Govoni, J.J., Hare, J.A., Davenport, E.D., Chen, M.H., Marancik, K.E., 2010. Mesoscale, cyclonic eddies as larval fish habitat along the Southeast United States shelf: A Lagrangian description of the zooplankton community. ICES J. Mar. Sci. 67, 403–411. https://doi.org/10.1093/icesjms/fsp269.

Grantham, H.S., Game, E.T., Lombard, A.T., et al., 2011. Accommodating dynamic oceanographic processes and pelagic biodiversity in marine conservation planning. PLoS ONE 6 (2), e16552. https://doi.org/10.1371/journal.pone.0016552.

Griffa, A., Kirwan, Jr, A., Mariano, A., Ozgokmen, T., Rossby, H. (Eds.), 2007. Lagrangian Analysis and Prediction of Coastal and Ocean Dynamics. Cambridge University Press, Cambridge. https://doi.org/10.1017/CBO9780511535901.

Haller, G., 2002. Lagrangian coherent structures from approximate velocity data. Phys. Fluids 14 (6), 1851–1861. https://doi.org/10.1063/1.1477449.

Haller, G., 2011. A variational theory of hyperbolic Lagrangian Coherent Structures. Phys. D: Nonlinear Phenom. 240 (7), 574–598. https://doi.org/10.1016/j.physd.2010.11.010.

Haller, G., 2015. Lagrangian coherent structures. Ann. Rev. Fluid Mech. 47 (1), 137. https://doi.org/10.1146/annurev-fluid-010313-141322.

Hare, J.A., Cowen, R.K., 1996. Transport mechanisms of larval and pelagic juvenile bluefish (Pomatomus saltatrix) from South Atlantic Bight spawning grounds to Middle Atlantic Bight nursery habitats. Limnol. Oceanogr. 41, 1264–1280. https://doi.org/10.4319/lo.1996.41.6.1264.

Harrison, C.S., Glatzmaier, G.A., 2012. Lagrangian coherent structures in the California Current System — sensitivities and limitations. Geophys. Astrophys. Fluid Dyn. 106, 22–44. https://doi.org/10.1080/03091929.2010.532793.

Harrison, C.S., Siegel, D.A., Mitarai, S., 2013. Filamentation and eddy−eddy interactions in marine larval accumulation and transport. Mar. Ecol. Prog. Ser. 472, 27–44. https://doi.org/10.3354/meps10061.

Hashimoto, M., Kidokoro, H., Suyama, S., Fuji, T., Miyamoto, H., Naya, M., Vijai, D., Ueno, Y., Kitakado, T., 2020. Comparison of biomass estimates from multiple stratification approaches in a swept area method for Pacific saury Cololabis saira in the western North Pacific. Fish. Sci. 86 (3), 445–456. https://doi.org/10.1007/s12562-020-01407-3.

Haza, A.C., Özgökmen, T.M., Hogan, P., 2016. Impact of submesoscale on surface material distribution in a Gulf of Mexico mesoscale eddy. Ocean Model. 107, 28–47. https://doi.org/10.1016/j.ocemod.2016.10.002.

Hernández-Carrasco, I., Alou-Font, E., Dumont, P.-A., et al., 2020. Lagrangian flow effects on phytoplankton abundance and composition along filament-like structures. Prog. Oceanogr. 189, 102469 https://doi.org/10.1016/j.pocean.2020.102469.

Hernández-Carrasco, I., Orfila, A., Rossi, V., et al., 2018. Effect of small scale transport processes on phytoplankton distribution in coastal seas. Sci. Rep. 8, 8613. https://doi.org/10.1038/s41598-018-26857-9.

Hilborn, R., 2007. Managing fisheries is managing people: what has been learned? Fish Fish 8, 285–296. https://doi.org/10.1111/j.1467-2979.2007.00263_2.x.

Hobday, A.J., Hartog, J.R., Spillman, C.M., Alves, O., 2011. Seasonal forecasting of tuna habitat for dynamic spatial management. Can. J. Fish. Aquat. Sci. 68, 898–911. https://doi.org/10.1139/f2011-031.

Hobday, A.J., Hartog, J.R., 2014. Derived ocean features for dynamic ocean management. Oceanography 27 (4), 134–145. https://doi.org/10.5670/oceanog.2014.92.

Hsu, J., Chang, Y.J., Kitakado, T., Kai, M., Li, B., et al., 2021. Evaluating the spatiotemporal dynamics of Pacific saury in the Northwestern Pacific Ocean by using a geostatistical modelling approach. Fish. Res. 235, 105821 https://doi.org/10.1016/j.fishres.2020.105821.

Hyrenbach, K.D., Forney, K.A., Dayton, P.K., 2000. Marine Protected Areas and ocean basin management. Aquat. Conserv.: Mar. Freshw. Ecosyst. 10, 437–458. https://doi.org/10.1002/1099-0755(200011/12)10:6<437::AID-AQC425>3.0.CO;2-Q.

Irigoien, X., et al., 2014. Large mesopelagic fish biomass and trophic efficiency in the open ocean. Nat. Commun. 5, 3271. https://doi.org/10.1038/ncomms4271.

Ito, D., Kodama, T., Shimizu, Y., Setou, T., Hidaka, K., Ambe, D., Sogawa, S., 2023. Frontogenesis elevates the maximum chlorophyll a concentration at the subsurface near the Kuroshio during well-stratified seasons. J. Geophys. Res.: Oceans 128, e2022JC018940. https://doi.org/10.1029/2022JC018940.

Kahru, M., Di Lorenzo, E., Manzano-Sarabia, M., Mitchell, B.G., 2012. Spatial and temporal statistics of sea surface temperature and chlorophyll fronts in the California current. J. Plankton Res. 34, 749–760. https://doi.org/10.1093/plankt/fbs010.

Kasai, A., Kimura, S., Nakata, N., Okazaki, Y., 2002. Entrainment of coastal water into a frontal eddy of the Kuroshio and its biological significance. J. Mar. Syst. 37, 185–198. https://doi.org/10.1016/S0924-7963(02)00201-4.

Keating, S.R., Smith, K.S., Kramer, P.R., 2011. Diagnosing lateral mixing in the upper ocean with virtual tracers: Spatial and temporal resolution dependence. J. Phys. Oceanogr. 41 (8), 1512–1534. https://doi.org/10.1175/2011JPO4580.1.

Kida, S., Mitsudera, H., Aoki, S., Guo, X., Ito, S.-I., et al., 2015. Oceanic fronts and jets around Japan: a review. J. Oceanogr. 71 (5), 469–497. https://doi.org/10.1007/s10872-015-0283-7.

Kulik, V., Katugin, O., Baitaliuk, A., 2020a. CPUE Standardization for the Pacific Saury Russian Catches in the Northwest Pacific Ocean. Technical Report, Small Scientific Committee on Pacific Saury. Japan, Tokyo, North Pacific Fisheries Commission.

Kulik, V.V., Prants, S.V., Uleysky, M.Yu, Budyansky, M.V., 2022. Lagrangian characteristics in the western North Pacific help to explain variability in Pacific saury fishery. Fish. Res. 252, 106361 https://doi.org/10.1016/j.fishres.2022.106361.

Kulik, V.V., Varkentin, A.I., Il'in, O.I., 2020b. Standardization of catches per pollock effort in the northern part of the Sea of Okhotsk, taking into account some environmental factors. Izv. TINRO 200 (4), 819–836. https://doi.org/10.26428/1606-9919-2020-200-819-836 (in Russian with English abstract.

Kuroda, H., Yokouchi, K., 2017. Interdecadal decrease in potential fishing areas for Pacific saury off the southeastern coast of Hokkaido, Japan. Fish. Oceanogr. 26 (4), 439–454. https://doi.org/10.1111/fog.12207.

Lascelles, B.G., Langham, G.M., Ronconi, R.A., Reid, J.B., 2012. From hotspots to site protection: Identifying Marine Protected Areas for seabirds around the globe. Biol. Cons. 156, 5–14. https://doi.org/10.1016/j.biocon.2011.12.008.

Le Févre, J., 1987. Aspects of the biology of frontal systems. Adv. Mar. Biol. 23, 163–299. https://doi.org/10.1016/s0065-2881(08)60109-1.

Legeckis, R., 1978. A survey of worldwide sea surface temperature fronts detected by environmental satellites. J. Geophys. Res 83 (C9), 4501–4522. https://doi.org/10.1029/JC083iC09p04501.

Lehahn, Y., d'Ovidio, F., Koren, I., 2018. A satellite-based Lagrangian view on phytoplankton dynamics. Ann. Rev. Mar. Sci. 10 (1), 99. https://doi.org/10.1146/annurev-marine-121916-063204.

Lehahn, Y., d'Ovidio, F., Lévy, M., Heifetz, E., 2007. Stirring of the northeast Atlantic spring bloom: A Lagrangian analysis based on multisatellite data. C08005 J. Geophys. Res. Oceans 112 (C8). https://doi.org/10.1029/2006JC003927.

Lévy, M., Ferrari, R., Franks, P.J.S., Martin, A.P., Riviere, P., 2012. Bringing physics to life at the submesoscale. L14602 Geophys. Res. Lett. 39 (14). https://doi.org/10.1029/2012gl052756.

Lévy, M., Franks, P.J.S., Smith, K.S., 2018. The role of submesoscale currents in structuring marine ecosystems. Nat. Commun. 9 (1), 4758. https://doi.org/10.1038/s41467-018-07059-3.

Li, J., Cui, X., Tang, F., Fan, W., Han, Z., Wu, Z., 2023. Effects of Kuroshio and Mesoscale Eddy on Fishing Ground Gravity of Neon Flying Squid Ommastrephes bartramii in Northwest Pacific Ocean. J. Mar. Sci. Eng. 11, 966. https://doi.org/10.3390/jmse11050966.

Lipphardt, Jr, B.L., Small, D., Kirwan, Jr.A.D., Wiggins, S., et al., 2006. Synoptic Lagrangian maps: Application to surface transport in Monterey Bay. J. Mar. Res. 64, 221–247. https://doi.org/10.1357/002224006777606461.

Liu, D., Wang, Y., Wang, Y., Keesing, J.K., 2018. Ocean fronts construct spatial zonation in microfossil assemblages. Glob. Ecol. Biogeogr. 27, 1225–1237. https://doi.org/10.1111/geb.12779.

Logerwell, E.A., Smith, P.E., 2001. Mesoscale eddies and survival of late stage Pacific sardine (Sardinops sagax) larvae. Fish. Oceanogr. 10, 13–25. https://doi.org/10.1046/j.1365-2419.2001.00152.x.

Mangolte, I., Lévy, M., Haëck, C., Ohman, M.D., 2023. Sub-frontal niches of plankton communities driven by transport and trophic interactions at ocean fronts. Biogeosciences 20, 3273. https://doi.org/10.5194/bg-20-3273-2023.

Manso-Narvarte, I., Caballero, A., Hernandez-Carrasco, I., Orfila, A., et al., 2023. Effect of circulation at early life stages of European anchovy in the Bay of Biscay from observational data and a Lagrangian approach. J. Mar. Syst. 242, 103938 https://doi.org/10.1016/j.jmarsys.2023.103938.

Markina, N.P., Chernyavskii, V.I., 1984. Quantitative distribution of plankton and benthos in the Sea of Okhotsk. Izv. Tikhookean. Nauchno-Issled. Inst. Rybn. Khoz. Okean. 109, 109–119.

Martin, A., 2003. Phytoplankton patchiness: the role of lateral stirring and mixing. Progr. Oceanogr. 57, 125–174. https://doi.org/10.1016/S0079-6611(03)00085-5.

Martin, A., Richards, K., Bracco, A., Provenzale, A., 2002. Patchy productivity in the open ocean, 9-1 Glob. Biogeochem. Cycles 16. https://doi.org/10.1029/2001GB001449.

Mendoza, C., Mancho, A.M., 2010. Hidden Geometry of Ocean Flows. Phys. Rev. Lett. 105, 038501 https://doi.org/10.48550/arXiv.1003.0368.

Miller, P.I., 2009. Composite front maps for improved visibility of dynamic sea-surface features on cloudy SeaWiFS and AVHRR data. J. Mar. Syst. 78, 327–336. https://doi.org/10.1016/j.jmarsys.2008.11.019.

Miller, P.I., Christodoulou, S., 2014. Frequent locations of oceanic fronts as an indicator of pelagic diversity: Application to marine protected areas and renewables. Mar. Policy 45, 318–329. https://doi.org/10.1016/j.marpol.2013.09.009.

Morales-Márquez, V., Hernández-Carrasco, I., Fox-Kemper, B., Orfila, A., 2023. Ageostrophic contribution by the wind and waves induced flow to the lateral stirring in the Mediterranean Sea. J. Geophys. Res.: Oceans 128, e2022JC019135. https://doi.org/10.1029/2022JC019135.

Murawski, S.A., Wigley, S.E., Fogarty, M.J., Rago, P.J., Mountain, D.G., 2005. Effort distribution and catch patterns adjacent to temperate MPAs. ICES J. Mar. Sci. 62, 1150–1167. https://doi.org/10.1016/j.icesjms.2005.04.005.

Myers, R.A., Drinkwater, K., 1989. The influence of Gulf Stream warm core rings on recruitment of fish in the northwest Atlantic. J. Mar. Res. 47 (3), 635–656. https://doi.org/10.1357/002224089785076208.

Nakamura, T., Toyoda, T., Ishikawa, Y., Awaji, T., 2006. Enhanced ventilation in the Okhotsk Sea through tidal mixing at the Kuril Straits. Deep-Sea Res. Part I 53, 425–448. https://doi.org/10.1016/j.dsr.2005.12.006.

Nauman, E.B., 2008. Residence Time Theory. Ind. Eng. Chem. Res. 47 (10), 3752–3766. https://doi.org/10.1021/ie071635a.

Nishikawa, H., et al., 2021. Surface water pathways in the subtropical–subarctic frontal zone of the western North Pacific. Prog. Oceanogr. 199 (12), 102691 https://doi.org/10.1016/j.pocean.2021.102691.

Novikov, Y.V., Slobodskoy, E.V., Shevtsov, G.A., 2007. Influence of oceanological conditions on the distribution and biological features of the mass squid species in the South Kuril region. Oceanology 47 (2), 238–244. https://doi.org/10.1134/s0001437007020105.

Ohshima, K.I., Nakanowatari, T., Riser, S., Wakatsuchi, M., 2010. Seasonal variation in the in- and outflow of the Okhotsk Sea with the North Pacific. Deep-Sea Res. Part II 57 (13–14), 1247–1256. https://doi.org/10.1016/j.dsr2.2009.12.012.

Olson, D.B., Backus, R.H., 1985. The concentrating of organisms at fronts: A coldwater fish and a warm-core Gulf Stream ring. J. Mar. Res. 43 (1), 113–137. https://doi.org/10.1357/002224085788437325.

Olson, D., Hitchcock, G., Mariano, A., Ashjian, C., Peng, G., Nero, R., Podesta, G., 1994. Life on the edge: Marine life and fronts. Oceanography 7 (2), 52–60. https://doi.org/10.5670/oceanog.1994.03.

Onink, V., Wichmann, D., Delandmeter, P., Van Sebille, E., 2019. The role of Ekman currents, geostrophy, and Stokes drift in the accumulation of floating microplastic. J. Geophys. Res.: Oceans 124, 1474–1490. https://doi.org/10.1029/2018JC014547.

Ottino, J.M., 1989. The Kinematics of Mixing: Stretching, Chaos, and Transport. Cambridge Texts in Applied Mathematics (3). U.K., Cambridge, Cambridge University Press.

Owen, R.W., 1981. Fronts and eddies in the sea: Mechanisms, interactions and biological effects. In: Longhurst, A.R. (Ed.), Analysis of Marine Ecosystems. Academic Press Inc, London, pp. 197–233.

Palacios, D.M., Bograd, S.J., Foley, D.G., Schwing, F.B., 2006. Oceanographic characteristics of biological hot spots in the north Pacific: A remote sensing perspective. Deep Sea Res. Part II 53 (3–4), 250–269. https://doi.org/10.1016/j.dsr2.2006.03.004.

Pierrehumbert, R.T., 1991. Chaotic mixing of tracer and vorticity by modulated travelling rossby waves. Geophys. Astrophys. Fluid Dyn. 58 (1–4), 285–319. https://doi.org/10.1080/03091929108227343.

Polovina, J.J., Howell, E., Kobayashi, D.R., Seki, M.P., 2001. The transition zone chlorophyll front, a dynamic global feature defining migration and forage habitat for marine resources. Prog. Oceanogr. 49 (1–4), 469–483. https://doi.org/10.1016/s0079-6611(01)00036-2.

Ponomarev, V.I., Fayman, P.A., Prants, S.V., Budyansky, M.V., Uleysky, M.Yu, 2018. Simulation of mesoscale circulation in the Tatar Strait of the Japan Sea. Ocean Model. 126, 43–55. https://doi.org/10.1016/j.ocemod.2018.04.006.

Prants, S.V., 2013. Dynamical systems theory methods to study mixing and transport in the ocean. Phys. Scr. 87 (3), 038115 https://doi.org/10.1088/0031-8949/87/03/038115.

Prants, S.V., Andreev, A.G., Budyansky, M.V., Uleysky, M.Yu, 2015a. Impact of the Alaskan Stream flow on surface water dynamics, temperature, ice extent, plankton biomass and walleye pollock stocks in the eastern Okhotsk Sea. J. Mar. Syst. 151, 47–58. https://doi.org/10.1016/j.jmarsys.2015.07.001.

Prants, S.V., Budyansky, M.V., Uleysky, M.Y., 2014. Identifying Lagrangian fronts with favourable fishery conditions. Deep Sea Res. Part I 90, 27–35. https://doi.org/10.1016/j.dsr.2014.04.012.

Prants, S.V., Budyansky, M.V., Uleysky, M.Y., 2018. How eddies gain, retain and release water: A case study of a Hokkaido anticyclone. J. Geophys. Res 123, 2081–2096. https://doi.org/10.1002/2017jc013610.

Prants, S.V., Budyansky, M.V., Lobanov, V.B., Sergeev, A.F., Uleysky, M.Yu, 2020. Observation and Lagrangian analysis of quasi-stationary Kamchatka trench eddies. J. Geophys. Res. (Oceans) 125 (6) e2020JC016187. https://doi.org/10.1029/2020JC016187.

Prants, S.V., Budyansky, M.V., Ponomarev, V.I., Uleysky, M.Y., 2011. Lagrangian study of transport and mixing in a mesoscale eddy street. Ocean Model 38, 114–125. https://doi.org/10.1016/j.ocemod.2011.02.008.

Prants, S.V., Budyansky, M.V., Uleysky, M.Yu, Zhang, J., 2015b. Hyperbolicity in the ocean. Discontinuity, Nonlinear, Complex. 4 (3), 257–270. https://doi.org/10.5890/DNC.2015.09.004.

Prants, S.V., Budyansky, M.V., Uleysky, M.Y., Kulik, V.V., 2021. Lagrangian fronts and saury catch locations in the Northwestern Pacific in 2004–2019. J. Mar. Sys. 222, 103605 https://doi.org/10.1016/j.jmarsys.2021.103605.

Prants, S.V., Lobanov, V.B., Budyansky, M.V., Uleysky, M.Y., 2016. Lagrangian analysis of formation, structure, evolution and splitting of anticyclonic Kuril eddies. Deep Sea Res. Part I 109, 61–75. https://doi.org/10.1016/j.dsr.2016.01.003.

Prants, S.V., Uleysky, M.Y., Budyansky, M.V., 2012. Lagrangian coherent structures in the ocean favorable for fishery. Dokl. Earth Sci. 447 (1), 1269–1272. https://doi.org/10.1134/S1028334X12110062.

Prants, S.V., Uleysky, M.Y., Budyansky, M.V., 2017. Lagrangian Oceanography: Large-Scale Transport and Mixing in the Ocean. Physics of Earth and Space Environments. Springer Verlag, Berlin, New York. https://doi.org/10.1007/978-3-319-53022-2.

Qiu, B., 2002. The Kuroshio Extension System: Its Large-Scale Variability and Role in the Midlatitude Ocean-Atmosphere Interaction. J. Oceano 58, 57–75. https://doi.org/10.1023/A:1015824717293.

Reid, J.L., Brinton, E., Fleminger, A., Venrick, E.L., McGowan, J.A., 1978. Ocean circulation and marine life. In: Charnock, H., Deacon, G. (Eds.), Advances in Oceanography. Springer, Boston, pp. 65–130. https://doi.org/10.1007/978-1-4615-8273-1_3.

Russo, S., Torri, M., Patti, B., Musco, M., et al., 2022. Environmental Conditions along Tuna Larval Dispersion: Insights on the Spawning Habitat and Impact on Their Development Stages. Water 14, 1568. https://doi.org/10.3390/w14101568.

Rwawi, C., Hernandez-Carrasco, I., Sudre, F., Tedetti, M., Rossi, V., 2024. Transport patterns and hydrodynamic context of the MERITE-HIPPOCAMPE cruise: Implications for contaminants distribution and origin. Mar. Poll. Bull. 198, 115743 https://doi.org/10.1016/j.marpolbul.2023.115743.

Saitoh, S., Kosaka, S., Iisaka, J., 1986. Satellite infrared observations of Kuroshio warmcore rings and their application to study of Pacific saury migration. Deep Sea Res. A. 33 (11–12), 1601–1615. https://doi.org/10.1016/0198-0149(86)90069-5.

Sakurai, Y., 2007. An overview of the Oyashio ecosystem. Deep Sea Res. Part II 54, 2526–2542. https://doi.org/10.1016/j.dsr2.2007.02.007.

Samko, E.V., Bulatov, N.V., Kapshiter, A.V., 2007. Characteristics of anticyclonic eddies of various origin and their impact on the fishing of the saury and neon flying squid to the southeast of Hokkaido. Sovrem. Probl. Distantsionnogo Zondirovaniya Zemli Kosm. 4 (1), 357–369.

Sanial, V., van Beek, P., Lansard, B., d'Ovidio, F., et al., 2014. Study of the phytoplankton plume dynamics off the Crozet Islands (Southern Ocean): A geochemical-physical coupled approach. J. Geophys. Res. Oceans 119 (4), 2227–2237. https://doi.org/10.1002/2013jc009305.

Scales, K.L., et al., 2018. Fisheries bycatch risk to marine megafauna is intensified in Lagrangian coherent structures. PNAS 115 (28), 7362–7367. https://doi.org/10.1073/pnas.1801270115.

Scales, K.L., Miller, P.I., Hawkes, L.A., Ingram, S.N., Sims, D.W., Votier, S.C., 2014. Review: On the Front Line: frontal zones as priority at-sea conservation areas for mobile marine vertebrates. J. Appl. Ecol. 51 (6), 1575–1583. https://doi.org/10.1111/1365-2664.12330.

Schmid, M.S., Cowen, R.K., Robinson, K., Luo, J.Y., Briseno-Avena, C., Sponaugle, S., 2020. Prey and predator overlap at the edge of a mesoscale eddy: Fine-scale, in-situ distributions to inform our understanding of oceanographic processes. Sci. Rep. 10, 921. https://doi.org/10.1038/s41598-020-57879-x.

Ser-Giacomi, E., Baudena, A., Rossi, V., et al., 2021. Lagrangian betweenness as a measure of bottlenecks in dynamical systems with oceanographic examples. Nat. Commun. 12, 4935. https://doi.org/10.1038/s41467-021-25155-9.

Shadden, S.C., Lekien, F., Marsden, J.E., 2005. Definition and properties of Lagrangian coherent structures from finite-time Lyapunov exponents in two-dimensional aperiodic flows. Phys. D. 212, 271–304. https://doi.org/10.1016/j.physd.2005.10.007.

Shchepetkin, A.F., McWilliams, J.C., 2005. The regional oceanic modeling system (ROMS): a split-explicit, free-surface, topography-following-coordinate oceanic model. Ocean Model 9, 347–404. https://doi.org/10.1016/j.ocemod.2004.08.002.

Shulzitski, K., Sponaugle, S., Hauff, M., Walter, K., D'Alessandro, E.K., Cowen, R.K., 2015. Close encounters with eddies: Oceanographic features increase growth of larval reef fishes during their journey to the reef. Biol. Lett. 11, 20140746. https://doi.org/10.1098/rsbl.2014.0746.

Shulzitski, K., Sponaugle, S., Hauff, M., Walter, K., Cowen, R.K., 2016. Encounter with mesoscale eddies enhances survival to settlement in larval coral reef fishes. Proc. Natl. Acad. Sci. U. S. A. 113, 6928–6933. https://doi.org/10.1073/pnas.1601606113.

Snyder, S., Franks, P.J.S., Talley, L.D., Xu, Y., Kohin, S., 2017. Crossing the line: Tunas actively exploit submesoscale fronts to enhance foraging success. Limnol. Oceanogr. Lett. 2, 187–194. https://doi.org/10.1002/lol2.10049.

Sournia, A., 1994. Pelagic biogeography and fronts. Prog. Oceanogr. 34, 109–120. https://doi.org/10.1016/0079-6611(94)90004-3.

Sugimoto, T., Tameishi, H., 1992. Warm-core rings, streamers and their role on the fishing ground formation around Japan. Deep Sea Res. A 39, S183–S201. https://doi.org/10.1016/S0198-0149(11)80011-7.

Suthers, I.M., Schaeffer, A., Archer, M., Roughan, M., Griffin, D.A., Chapman, C.C., Sloyan, B.M., Everett, J.D., 2023. Frontal eddies provide an oceanographic triad for favorable larval fish habitat. Limnol. Oceano 68, 1019–1036. https://doi.org/10.1002/lno.12326.

Tew Kai, E., Rossi, V., Sudre, J., Weimerskirch, H., Lopez, C., Hernandez-Garcia, E., Marsac, F., Garçon, V., 2009. Top marine predators track Lagrangian coherent structures. PNAS 106, 8245–8250. https://doi.org/10.1073/pnas.0811034106.

Tseng, Sun, C.-T., Belkin, C.-L., Yeh, I.M., et al., 2014. Sea surface temperature fronts affect distribution of Pacific saury (Cololabis saira) in the Northwestern Pacific Ocean. Deep Sea Res. Part II 107, 15–21. https://doi.org/10.1016/j.dsr2.2014.06.001.

Uda, M., 1938. Researches on "Siome" or current rip in the seas and oceans. Geophys. Mag. 11, 307–372.

Ullman, D.S., Cornillon, P.C., 2000. Evaluation of front detection methods for satellite-derived sst data using in situ observations. J. Atmos. Ocean. Technol. 17, 1667–1675. https://doi.org/10.1175/1520-0426(2000)017<1667:EOFDMF>2.0.CO;2.

van Sebille, E., Griffies, S.M., Abernathey, R., Adams, T.P., Berloff, P., Biastoch, A., Zika, J., D, 2018. Lagrangian ocean analysis: Fundamentals and practices. Ocean Model. 121, 49–75. https://doi.org/10.1016/j.ocemod.2017.11.008.

Watson, J.R., Fuller, E.C., Castruccio, F.S., Samhouri, J.F., 2018. Fishermen follow finescale physical ocean features for finance. Front. Mar. Sci. 5, 46. https://doi.org/10.3389/fmars.2018.00046.

Weimerskirch, H., Le Corre, M., Jaquemet, S., Potier, M., Marsac, F., 2004. Foraging strategy of a top predator in tropical waters: great frigatebirds in the Mozambique Channel. Mar. Ecol. Prog. Ser. 275, 297–308. https://doi.org/10.3354/meps275297.

Wiggins, S., 1992. Chaotic Transport in Dynamical Systems. Book series Interdisciplinary Applied Mathematics. Springer, New York. https://doi.org/10.1007/978-1-4757-3896-4.

Woodson, C.B., Litvin, S.Y., 2015. Ocean fronts drive marine fishery production and biogeochemical cycling. PNAS 112, 1710–1715. https://doi.org/10.1073/pnas.1417143112.

Xing, Q., Yu, H., Wang, H., Yu, H., 2023. A sliding-window-threshold algorithm for identifying global mesoscale ocean fronts from satellite observations. Progr. Oceano 216, 103072. https://doi.org/10.1016/j.pocean.2023.103072.

Yasuda, I., 2003. Hydrographic structure and variability in the Kuroshio-Oyashio transition areas. J. Oceano 59, 389–402. https://doi.org/10.1023/A:1025580313836.

Yasuda, I., Watanabe, Y., 1994. On the relationship between the Oyashio front and saury fishing grounds in the north-western Pacific: a forecasting method for fishing ground locations. Fish. Oceanogr. 3 (3), 172–181. https://doi.org/10.1111/j.1365-2419.1994.tb00094.x.